Multi-fold increase in rainforests tipping risk beyond 1.5-2⁰C warming

Chandrakant Singh[1,2,3,*], Ruud van der Ent[4], Ingo Fetzer[1,2,5], Lan Wang-Erlandsson[1,2,5]

[1]Stockholm Resilience Centre, Stockholm University, Stockholm, Sweden

[2]Bolin Centre for Climate Research, Stockholm University, Stockholm, Sweden

[3]Department of Space, Earth and Environment, Chalmers University of Technology, Gothenburg, Sweden

[4]Department of Water Management, Faculty of Civil Engineering and Geosciences, Delft University of Technology, Delft, The Netherlands

[5]Potsdam Institute for Climate Impact Research, Potsdam, Germany

*Corresponding author; E-mail: chandrakant.singh@su.se, chandrakant.singh@chalmers.se

ORCID

Chandrakant Singh: http://orcid.org/0000-0001-9092-1855

Ruud van der Ent: https://orcid.org/0000-0001-5450-4333

Ingo Fetzer: http://orcid.org/0000-0001-7335-5679

Lan Wang-Erlandsson: http://orcid.org/0000-0002-7739-5069

Abstract. Tropical rainforests rely on their root systems to access moisture stored in soil during wet periods for use during dry periods. When this root-zone soil moisture is inadequate to sustain a forest ecosystem, they transition to a savanna-like state, losing their native structure and functions. Yet the influence of climate change on ecosystem's root-zone soil moisture storage and their impact on rainforest ecosystems remain uncertain. This study assesses the future state of rainforests and the risk of forest-to-savanna transitions in South America and Africa under four shared socioeconomic pathways (SSP1-2.6, SSP2-4.5, SSP3-7.0, and SSP5-8.5). Using a mass-balance-based empirical understanding of root zone storage capacity (S_r), defined as the maximum volume of root zone soil moisture per unit area accessible to vegetation's roots for transpiration, we project how rainforest ecosystems will respond to future climate changes. We find that under the end-of-the-21st-century climate, nearly one-third of the total forest area will be influenced by climate change. As the climate warms, forests will require a larger S_r than they do under the current climate to sustain their ecosystem structure and functions, making them more water-limited. Meanwhile, recovering to a less water-limited state gradually diminishes. Furthermore, warming beyond 1.5-2⁰C will significantly elevate the risk of a forest-savanna transition. In the Amazon, the forest area at risk of such a transition grows by about 1.7-5.8 times in size compared to their immediate lower warming scenario (e.g., SSP2-4.5 compared to SSP1-2.6). In contrast, the risk growth in the Congo is less substantial, ranging from 0.7-1.7 times. These insights underscore the urgent need to limit global surface temperature rise below the Paris Agreement to conserve rainforest ecosystems and associated ecosystem services.

1 Introduction

Tropical rainforests in the Amazon and Congo basins are critical to the Earth system since they store and sequester a large amount of carbon, host vast biodiversity, and regulate the global water cycle (Malhi et al., 2014). However, these forests are under severe pressure from climate change and land-use change (Davidson et al., 2012; Lewis et al., 2015; Malhi et al., 2008), which risk amplifying further warming and forest degradation (Lawrence et al., 2022). Climate change and land-use change lead to a decrease in precipitation, an increase in seasonality and atmospheric water demand (Malhi et al., 2014). This causes a deficit in soil moisture availability that inhibits plant growth (Singh et al., 2020; Wang-Erlandsson et al., 2022). Furthermore, climate-induced hydroclimatic changes, including the projected increases in drought frequency, severity, and duration (Dai, 2011; Liu et al., 2018), present imminent threats to the capacity of rainforests to maintain their native ecological structure and functions (i.e., forest resilience) (Bauman et al., 2022; Grimm et al., 2013; Jones et al., 2009).

Under water-deficit conditions, rainforests adapt by investing in their root systems to gain better access to soil moisture necessary to maintain their structure and functions (Singh et al., 2020, 2022). At the same time, the availability of surplus moisture at shallow depths minimises the need for ecosystems to invest in extensive (deeper and lateral) root systems (Bruno et al., 2006). Furthermore, forest ecosystems adapt to climate change by optimising water distribution through mechanisms such as hydraulic redistribution (Liu et al., 2020; Oliveira et al., 2005), enhancing water-use efficiency by regulating stomatal conductance, and even shredding leaves (Wolfe et al., 2016) to minimise moisture loss (Barros et al., 2019; Brum et al., 2019; Lammertsma et al., 2011). Despite their critical role, the dynamic influence of climate change on vegetation's rooting structure and subsoil moisture is challenging to measure at the ecosystem scale (Fan et al., 2017). Thus, understanding how moisture from wet periods is stored, transmitted, and lost from soil, and how it is accessed by vegetation during dry periods, is critical to the ecohydrology and resilience of terrestrial ecosystems under climate change.

However, such ecohydrological dynamics remain challenging to incorporate in Earth System Models (ESMs) (Lenton, 2011; Maslin and Austin, 2012; Valdes, 2011) – complex mathematical representations of Earth system processes and interactions across different biospheres. This limits ESM's capacity to simulate tipping points as an emergent property of the system (i.e., properties that emerge due to multiple interactions between several system components, and are not the property of an individual component) (Hirota et al., 2021; Reyer et al., 2015). This constraint is mainly due to our poor understanding of complex mechanisms governing the ecosystem, which are not well represented in ESMs. This includes a limited understanding of vegetation-climate feedbacks (Boulton et al., 2013, 2017; Chai et al., 2021), subsoil moisture availability (Cheng et al., 2017), adaptation dynamics (Yuan et al., 2022), the response time of forest ecosystems to climate change perturbations, and assumptions about future (i.e., prescribed) land-use change (Hurtt et al., 2020) in the ESMs. Furthermore, in the Earth system, some interactions still remain largely unknown, thereby making the prediction of (abrupt) forest-to-savanna transition (referring to changes in the dense-canopy structure of

forests to one that mimics an open-canopy structure similar to savanna; hereafter referred to as forest-savanna transition) challenging (Drijfhout et al., 2015; Hall et al., 2019; Koch et al., 2021).

To understand the extent of rainforest tipping risks, there is a need to assess and contrast the forest resilience consequences of low-emission and current commitment trajectories with the more commonly used high-emission scenario (Jehn et al., 2022). However, the risk of forest-savanna transitions under various possible climate future scenarios is relatively under-investigated. As a result of the conflicting findings and scenario-dependent uncertainties, the Intergovernmental Panel on Climate Change (IPCC) has only low confidence about the possible tipping of the Amazon forest by the end of the 21st century (Canadell et al., 2021). However, with mounting empirical evidence on how climate change influences rainforest ecosystems (Boulton et al., 2022; Küçük et al., 2022; Singh et al., 2020, 2022), the research on rainforest resilience loss has accelerated considerably in the recent decade (Ahlström et al., 2017; Huntingford et al., 2013). Yet, forest resilience is often assessed based on changes in forest carbon stocks (Huntingford et al., 2013; Parry et al., 2022) or precipitation (Hirota et al., 2011; Staal et al., 2020; Zemp et al., 2017); and rarely on the subsoil moisture availability of the ecosystem (Singh et al., 2022).

This study aims to assess the state of rainforests and the risk of a forest-savanna transition under the end of the 21st-century climate based on an empirical understanding of ecosystems' root zone storage dynamics. For this, we use mass-balance derived root zone storage capacity (S_r) – representing the maximum amount of soil moisture vegetation can access for transpiration (Gao et al., 2014; Singh et al., 2020; Wang-Erlandsson et al., 2016). Our use of S_r is grounded in its effectiveness in representing ecosystems' access to soil moisture and their ability to modify above-ground structures accordingly (de Boer-Euser et al., 2016; Singh et al., 2020; Stocker et al., 2023; Wang-Erlandsson et al., 2016). It should be noted that we refer to rainforest tipping as a forest-savanna transition 'risk' since the timing of such transitions depends on the stochastic fluctuations of other environmental factors, beyond just hydroclimate (e.g., fire, human influence, species composition) (Cole et al., 2014; Cooper et al., 2020; Higgins and Scheiter, 2012; Poorter et al., 2016). Therefore, to project if an ecosystem is a forest or has tipped to savanna in the future, we assume the hydroclimate projected by the end of the 21st century (i.e., 2086-2100) and ecosystem are in equilibrium. However, we do not account for the time required for ecosystems to reach their (long-term) equilibrium state, which previous studies suggest can take between 50-200 years after crossing the tipping point (Armstrong McKay et al., 2022).

2   Methodology

2.1   Study Area

This study focuses on forest ecosystems (i.e., excluding savanna/grassland and vegetation in human-influenced ecosystems) extending between 15°N–35°S for South America and Africa.

**2.2 Data**

This analysis uses both empirical and ESM-simulated datasets of precipitation and evaporation. Empirical datasets include remotely sensed and observation-corrected precipitation and evaporation time-series. Empirical precipitation estimates at daily timestep are obtained from the Climate Hazards Group InfraRed Precipitation with Station data (CHIRPS; 0.25^o resolution) (Funk et al., 2015). Furthermore, empirical evaporation is derived using an equally-weighted ensemble of three different datasets – (i) Breathing Earth System Simulator (BESS; 0.5^o resolution) (Jiang and Ryu, 2016) (ii) Penman-Monteith-Leuning (PML; 0.5^o resolution) (Zhang et al., 2016) and (iii) FLUXCOM-RS (0.083^o resolution) (Jung et al., 2019) – at monthly timestep. Here, evaporation represents the sum of all evaporated moisture from the soil, open water and vegetation, including interception and transpiration. We only selected evaporation datasets free from biome-dependent parameterisation (such as plant function types, stomatal conductance, and maximum root allocation depth) and soil layer depth (represents maximum depth of moisture uptake). Ultimately, all evaporation datasets are bilinearly interpolated to 0.25^o resolution and downscaled to daily timestep using ERA5 evaporation (0.25^o resolution) estimates (Hersbach et al., 2020). All empirical datasets are obtained for 2001-2012.

We also obtained precipitation and evaporation estimates from 33 ESMs (from 22 different institutes), which includes CMIP6-historical and four SSP scenario simulations (SSP1-2.6 leads to approx. 1.3-2.4^{o}C warming; SSP2-4.5 corresponds to 2.1-3.5^{o}C warming and is closest to the current trajectory according to the nationally determined contributions (Anon, 2015); SSP3-7.0 around 2.8-4.6^{o}C warming; and SSP5-8.5 represents 3.3-5.7^{o}C warming; ^{o}C warming represents an increase in mean global surface temperature change by the end of 21st century relative to 1850-1900 (IPCC, 2021) (Fig. 1; Table S1 and S2). The historical estimates are obtained at a monthly timestep for 2000-2014, and the estimates under different SSPs are obtained for 2086-2100. Though obtained estimates from different ESMs are at different spatial resolutions, we bilinearly interpolated them to 0.25^o for this analysis.

Finally, to minimise the influence of human activity and non-forest land cover on the natural water cycle, we utilised land-cover data to remove pixels with such features from our analysis. We began by removing human-influenced and non-forest land cover, such as savanna, grasslands, and water bodies, from Globcover, a global land-cover classification dataset by the European Space Agency (ESA) at 300m resolution (GlobCover land-use map, 2022). We then performed majority interpolation to convert the dataset to a 0.25^o resolution and to mask grid cells with less than 50% forest cover. This step ensured that only grid cells with over 50% forest cover were classified as forests for further analysis.
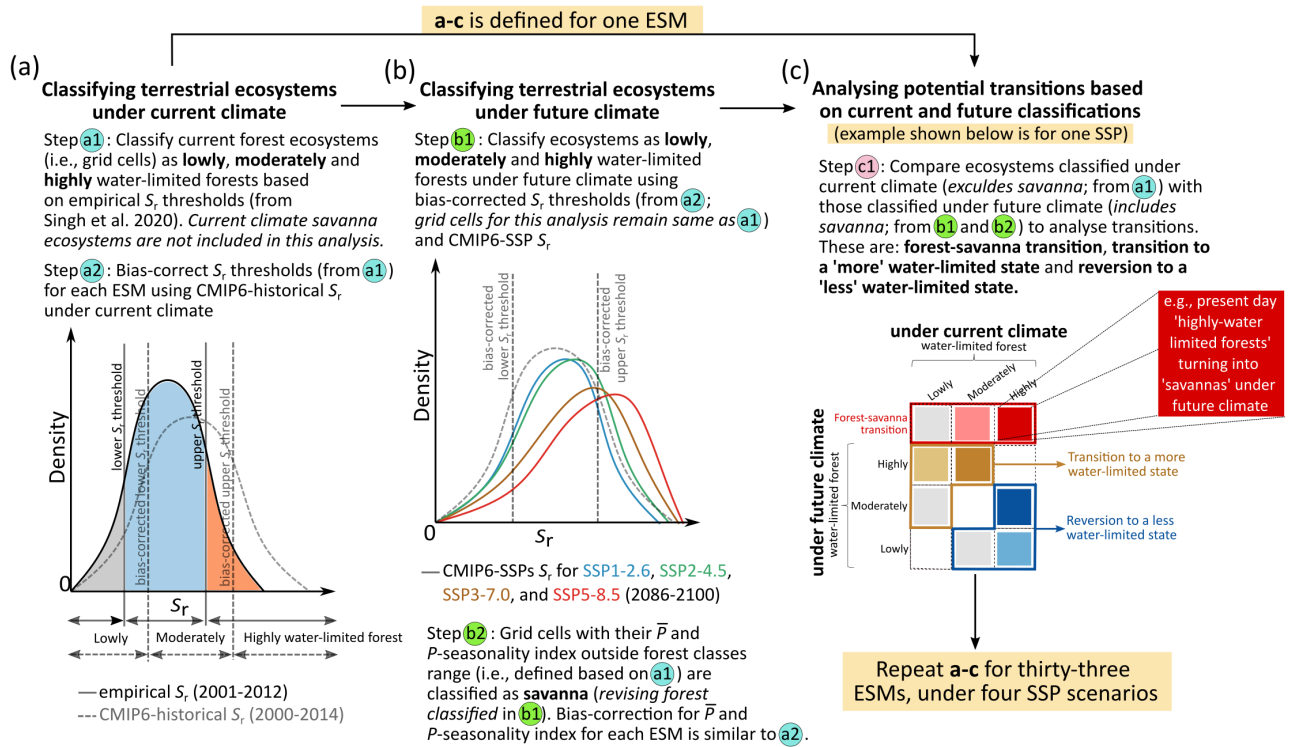
Figure 1: Methodological framework for analysing the potential transitions in tropical terrestrial ecosystems using empirical and CMIP6-Earth System Models (ESMs) hydroclimate estimates. (a) We use root zone storage capacity (S_r)-based classification thresholds (obtained from Singh et al., 2020) – calculated using empirical precipitation (P) and evaporation (E) estimates (Fig. S1; see Methodology section and Appendix A1) – to classify terrestrial ecosystems under the current climate. Savanna ecosystems under the current climate are excluded from this analysis. We bias-correct these S_r thresholds for all ESMs using the histogram equivalence method (Piani et al., 2010) (Table S1). **(b)** We then use these bias-corrected S_r thresholds to classify ecosystems under future climate conditions (Fig. S2 and S3). Furthermore, we use mean annual precipitation ($\overline{P}$) and P-seasonality index range (S_r-based forest classes from a) – as a proxy for ecosystem state – to revise our classification under future climate (Appendix A3 and Fig. S4). **(c)** We then analyse the potential transitions by comparing ecosystems classified under the current climate (analysed in a) with those classified under future climate (analysed in b) individually for all ESMs (Fig. S5 and S6). The transition analysis assumes that the vegetation and hydroclimate are in equilibrium, and does not account for the time required for transitions to occur. A detailed description is provided in the Methodology section. An exemplification of this methodological framework is shown in Fig. S7.

2.3   Root zone storage capacity-based framework for projecting forest transitions

Vegetation uptakes soil moisture from its roots; thus, the availability of root zone moisture is a key element that mediates the interaction between vegetation and climate (Brooks et al., 2015; Küçük et al., 2022; Rosas et al., 2019; Wang-Erlandsson et al., 2022). However, measuring soil- (such as texture and porosity) and root-characteristics (such as vertical and lateral extent and soil moisture uptake profiles) that influence access to subsoil moisture are challenging to measure at ecosystem scales (Bruno et al., 2006). Furthermore, land-system models tend to oversimplify the transfer and storage of water in root-zone due to insufficient knowledge about soil-vegetation-climate interactions (Albasha et al., 2015; Hildebrandt et al., 2016; Wang et al., 2004). In such cases, the mass-balance approach-based S_r provides a tangible and comprehensive understanding of ecosystem

5

162   access to moisture stored in the soil (de Boer-Euser et al., 2016; Gao et al., 2014; McCormick et al., 2021; Stocker

163   et al., 2023).

164

165   **2.3.1   Estimating mass-balance derived root zone storage capacity (S_r)**

166   Derived using the mass-balance approach, S_r represents the maximum amount of soil moisture accessed by

167   vegetation for transpiration (Singh et al., 2020; Wang-Erlandsson et al., 2016). This methodology calculates the

168   maximum extent of soil moisture within the reach of plant roots, assuming that ecosystems do not invest in

169   expanding their root-zone storage beyond what is necessary to bridge the maximum (accumulated) water-

170   deficit experienced by the vegetation during dry periods (i.e., periods in which evaporation is greater than

171   rainfall, irrespective of the seasons). This maximum annual accumulated water deficit ($D_{a,y}$) experienced by the

172   ecosystem is calculated using daily precipitation and evaporation estimates (Appendix A1 and Fig. A1). Subsoil

173   moisture beyond the reach of plant roots is primarily controlled by gravity-induced gradients (de Boer-Euser et

174   al., 2016) and is not available for transpiration. The rationale is that any extensive investment (i.e., more than

175   necessary) in root expansion would require carbon allocation and, thus, is inefficient from the perspective of

176   the plants (Gao et al., 2014; Schenk, 2008). Since, this approach does not rely on prior information about

177   vegetation, soil, or land cover-based, by using empirical (observation-based) datasets (Appendix A1 and Fig.

178   A1), we capture the dynamics of actual soil moisture available for the ecosystems (Wang-Erlandsson et al.,

179   2016). The detailed methodology for calculating S_r using precipitation and evaporation estimates is outlined in

180   Appendix A1.

181   In this mass-balance approach, S_r only represents a hydrological buffer essential for maintaining the

182   ecosystem's structure and functions (Gao et al., 2014; Wang-Erlandsson et al., 2016). However, other biotic and

183   abiotic factors, such as root morphology, soil depth, and geological formations, can physically restrict S_r by

184   limiting rooting depth, rooting structure, and the soil's water-holding capacity (Canadell et al., 1996; Jackson et

185   al., 1996; Schenk and Jackson, 2002) (Appendix A2). Additionally, soil properties like porosity or field capacity

186   could necessitate a deeper rooting strategy in different soil types (e.g., between sandy and clayey soil) to

187   achieve a comparable level of S_r to sustain the ecosystem under future climate (Kukal and Irmak, 2023).

188   However, this study assesses the impact of future climate change on the ecosystem's hydrological regime,

189   focusing on the changes to the ecosystem's equilibrium state. Therefore, the direct influence of soil and root

190   characteristics under future climate change on S_r (Appendix A2) and forest transitions falls outside our current

191   scope.

192

2.3.2   Determining root zone storage capacity thresholds for forest transitions

A recent study by Singh et al. (2020) demonstrated that S_r effectively represents an ecosystem's above-ground state (i.e., whether it is a forest or savanna) and its level of water–stress, based on root-zone moisture availability. In this study, we refine their terminology from 'water-stressed state' to 'water-limited state' to more precisely describe the effects of hydroclimatic conditions on forest ecosystems, specifically in terms of inhibiting plant growth based on subsoil moisture availability and the potential of them approaching the threshold of forest-savanna transition. According to Singh et al. (2020), in response to water-limited conditions, forests adapt their rooting strategies and modify their above-ground forest cover. These adaptations aim to allocate carbon in the most efficient way possible to maximise the hydrological benefits available to the ecosystem. They classified terrestrial ecosystems into four distinct categories based on the relationship between tree cover density and root zone storage capacity (S_r), illustrating the various drought coping strategies of ecosystems (detailed description provided in Singh et al., 2020):

i. **Lowly water-limited forest:** Dense forests (>70% tree cover) that receive ample rainfall (with daily precipitation exceeding evaporation year-round) results in a very low $D_{a,y}$. In such an environment, the top layer of the soil remains consistently damp, allowing for efficient soil moisture uptake through shallow roots (<1m; S_r and maximum rooting depth comparison in Singh et al., 2020), as vegetation typically utilises the shortest available pathway for moisture uptake (Bruno et al., 2006). Consequently, these forest ecosystems can sustain themselves with a low S_r (<100 mm).

ii. **Moderately water-limited forest:** Although these forests retain a dense structure (>65% tree cover), the increased precipitation seasonality (evaporation rates remain same as before) leads to a relatively higher $D_{a,y}$. This necessitates a greater investment in their rooting systems to access subsoil moisture for dry periods, with S_r for these ecosystems ranging between 100-400 mm in South America and 100-350 mm in Africa. Notably, this enhanced below-ground investment does not compromise the above-ground ecosystem structure.

iii. **Highly water-limited forest:** With further increase in precipitation seasonality (even negligible precipitation during dry seasons) and duration of dry period, forests need to maximize their S_r (maximum rooting depths typically between 15-20m). Maintaining ecosystems under these conditions is costly from a subsoil investment perspective (Schenk, 2008), with regions in South America and Africa showing S_r values as high as 750 mm and 450 mm, respectively. Consequently, these values represent the upper limits beyond which forest ecosystems cannot further enhance their S_r.

Possible mechanisms suggest that these trees adapt by shedding leaves to minimise moisture loss (Wolfe et al., 2016). However, this adaptation can reduce photosynthetic activity, leading to declines in root growth, and heightening the risk of mortality from hydraulic failures due to the unavailability of soil moisture at accessible depths (Guswa, 2008). Furthermore, accumulation of dry

227   leaves also perpetuates forest fires, thinning the ecosystem even further (tree cover can drop as low as

228   30%) (Nepstad et al., 1999). Although increased tree mortality reduces competition for water, enabling

229   some trees to survive, the heightened risk of hydraulic failures and forest fires makes these ecosystems

230   highly susceptible to transitioning to savanna.

231   iv.   **Savanna-grassland regime** (hereafter referred to as **savanna**): These ecosystems, typically

232   characterised by an open, grass-dominated structure (tree cover <40%), have both a lower water

233   availability and demand (both precipitation and evaporation are lower than in forest ecosystems). Thus,

234   requiring a lower hydrological buffer to sustain their structure and functions. For these ecosystems, S_r

235   values can be as low as 100 mm. Although tree species in this ecosystem can develop deep roots

236   (extending up to 20m), the majority of the root biomass is concentrated in the shallow soil layers (top

237   30–50 cm; shallow water uptake profile) (Nippert and Holdo, 2015; Schenk, 2008). This strategy allows

238   for completive moisture uptake between trees and grass species. This also suggests that, for savanna,

239   deeper roots don't always necessitate a high S_r.

240

241   The difference in S_r thresholds between both continents is due to the presence of water-use-efficient

242   C4 grasses in Africa (Still et al., 2003), which reduces the competitiveness for moisture uptake between tree

243   species and grasses – leading to a lesser need for extensive S_r in the African forest ecosystem (Singh et al., 2020).

244   Furthermore, these adaptation dynamics align with the alternative stable state theory (i.e., forest's stabilising

245   feedback under hydroclimatic changes and tipping risk beyond certain hydroclimatic extremes) (Hirota et al.,

246   2011), which makes S_r more representative of the transient state of the ecosystem than precipitation (Singh et

247   al., 2022). We, thus, use these mass-balance derived S_r thresholds to project rainforest transitions and tipping

248   risk under future climate change. A detailed description of how previous studies have projected rainforest

249   tipping (Table S3), and how S_r-based framework builds upon their shortcomings is mentioned in the

250   Supplement.

251

252   **2.3.3   Projecting forest transitions under future climate change**

253   To project forest transitions under future climate, we have to first classify forests based on S_r thresholds under

254   the current and future climate. Based on this classification, we analyse potential transition for each ESM and

255   aggregate the results (Fig. 1). We start by classifying forests under current climate following the approach by

256   Singh et al. (2020), which uses the (empirical) daily estimates of CHIRPS precipitation and ensemble evaporation

257   (2001-2012) (Appendix A1 and Sect. 2.3.2) (Fig. 1a). Since we are only interested in forest transitions, the

258   ecosystems classified as savanna under the current climate are excluded from this analysis.

259   Next, for classifying ecosystems under future climate scenarios, we follow the same mass-balance

260   approach (Appendix A1). However, since precipitation and evaporation estimates from ESMs do not align with

empirical estimates (Baker et al., 2021; McFarlane, 2011), we employ a bias-correction method. Specifically, we use a histogram equivalence method (Piani et al., 2010) to adjust empirical S_r thresholds to comparable CMIP6 S_r thresholds for various ESMs (Table S1). This involves, first, calculating S_r using CMIP6-historical precipitation and evaporation estimates between 2000-2014 (Appendix A1 and Fig. S8). We then determine a percentile-equivalent S_r thresholds for each of the thirty-three CMIP6-ESMs under the current climate. For example, if an empirical S_r of 100 mm corresponds to the 10th percentile (n = 20% of total pixels), we find the 10th percentile in the CMIP6-historically S_r, which may be higher or lower than 100 mm for each ESM (Fig. 1 and Table S1). These percentile-equivalent S_r thresholds are then used to classify ecosystems both under current (CMIP6-hsitorical; 2000-2014) and future climate (CMIP6-SSPs; 2086-2100) (Fig. 1b). Classifying savanna under future climate requires an additional step as outlined in Appendix A3.

Ultimately, we evaluate potential transitions by comparing ecosystems classified under current climate conditions (*this excludes savanna*) with those under future climate conditions (*this includes savanna*) (Sect. 2.3.2). These transitions are divided into three distinct categories (Fig. 1c and Fig. A2):

   i. **Forest-savanna transition:** This refers to current climate forest ecosystems that risk transitioning to a savanna under future climate change.

   ii. **Transition to a more water-limited state:** This includes ecosystems that shift to a higher water-limited state in the future. For example, if a forest currently classified as lowly water-limited transitions to either a moderately or highly water-limited state in the future, it would fall under this category.

   iii. **Reversion to a less water-limited state:** This includes ecosystems that shift to a lower water-limited state in the future.

To aggregate the results from all ESMs, grid cells with > 50% convergence are referred to as 'moderate-high model agreement', 20-50% as 'moderate model agreement' and ≤ 20% as 'low model agreement'. In the Results section, we primarily discuss estimates from scenarios >20% and >50% model convergence. While a threshold of >20% may seem low given the total number of ESMs analysed, it is important to recognise the variable and often limited capabilities of these ESMs, particularly in simulating biophysical interaction and emerging properties due to our limited understanding of the Earth system (Lenton et al., 2019; Stevens and Bony, 2013). Opting for a majority-based consensus in ESMs could overlook critical tipping risks identified by a minority of models, which might provide insights as valid as those from more widely agreeing models (Arora et al., 2023; Reyer et al., 2015).

2.4 Sensitivity analyses

Our methodology operates under two key assumptions: (i) the empirically derived S_r thresholds remain valid in the future, and (ii) the hydroclimatic estimates projected by ESMs accurately represent the actual climate, even

though these models have prescribed land-cover (Hurtt et al., 2020). To address the uncertainties related to the first assumption, we conduct four sensitivity analyses to assess the robustness of our analysis: (a) assuming that the regions exceeding the 99th percentile S_r are prone to a forest-savanna transition, as high S_r investment could be unrealistic from the perspective of plants under future climate change, (b) evaluating forest transitions using three different evaporation datasets, (c) assessing forest transitions under 10- and 40-year drought return periods, and (d) adjusting the forest-savanna transition thresholds.

Regarding the second assumption, we explicitly apply this methodology across a wide range of available ESMs under four SSP scenarios to identify consistencies and discrepancies in the results. Additionally, the discrepancies between the prescribed land-use and the forest transitions derived from our methodology, as well as the implications of these assumptions are detailed in the Discussion section.

3 Results

We find that under future climate conditions (2086-2100), considering >50% models' agreement, about one-fourth of the forests in both South America and Africa are projected to transition (Fig. 2b-g). With >20% models' agreement, these transitions are projected to occur for about three-fourths of the forests for both continents. Considering a lower threshold for models' agreement causes double or triple counting of some transitions (Fig. 2b-g). To minimise this in further analyses, we only consider >50% models' agreement for forests that transition to a more and less water-limited state. Furthermore, because (abrupt) forest-savanna transitions are under-represented in ESMs (Drijfhout et al., 2015; Lenton, 2011; Maslin and Austin, 2012; Valdes, 2011), we consider >20% models' agreement for them. Considering this, we not only reduce the overlap to <0.4% of the total forest area (Fig. S9), but we also maximise highlighting forest-savanna transition risk for both continents.

We find that the risk of forest-savanna transitions mainly occurs in the Guiana Shield of South America, and the southern and south-eastern regions of Africa (Fig. 3). Compared to Africa, forest-savanna transitions are more prominent in South America under warmer climates (i.e., higher SSPs; Fig. 2b and 3). Our analysis reveals that the extent of forest-savanna transitions in South America decreases from almost 1.32×10^6 km^2 (16.3% of total forest area in South America) under the highest emission scenario to 0.04×10^6 km^2 (0.5%) under the lowest emission scenario (Fig. 2b). Interestingly, for Africa, the extent of forest-savanna transition did not change much for different SSPs, i.e., (median) 0.25×10^6 km^2 with a maximum deviation of $\pm 0.11 \times 10^6$ km^2 (minimum and maximum extent of transition between 3-6.6% of total forest area in Africa) (Fig. 2c).

When comparing the changes in forest-savanna transition risk areas relative to their immediate lower warming scenarios, we find considerable increases for South America. The highest relative growth of approximately 5.75 times is observed between SSP1 and SSP2, with the forest area under risk increasing from 0.04×10^6 km^2 to 0.23×10^6 km^2, respectively. It increases by 3.48 times from SSP2 to SSP3 (0.23×10^6 km^2 to 0.80×10^6 km^2), and by 1.65 times from SSP3 to SSP5 (0.80×10^6 km^2 to 1.32×10^6 km^2). For Africa, however,

10

329   the increases are more modest: the risk grows by 1.29 times from SSP1 to SSP2 (0.17×10^6
330   km^2 to 0.22×10^6 km^2), by 1.63 times from SSP2 to SSP3 (0.22×10^6 km^2 to 0.36×10^6 km^2), and is observed to decrease by 0.72
331   times from SSP3 to SSP5 (0.36×10^6 km^2 to 0.26×10^6 km^2).

332   By evaluating changes to their hydroclimate, we find that under warmer climates, forest-savanna
333   transition regions in both continents are projected to experience a decrease in precipitation. Furthermore, we
334   observe an increase in precipitation seasonality for South America, whereas Africa shows a decrease (Fig. S12).
335   Here, an increase in precipitation seasonality (seasonal variability in precipitation over the year) creates water-
336   limited conditions for the ecosystem. In contrast, a decrease in seasonality and precipitation in Africa
337   corresponds to a lower moisture availability altogether. Nevertheless, for both these continents, this transition
338   seems to occur for the previously highly water-limited forests under the current climate, followed by
339   moderately, with the least contribution from lowly water-limited forests (Fig. 3). This highlights the looming risk
340   on highly water-limited forests to experience a forest-savanna transition under warmer climates.

341   Forests that transition to a 'more' water-limited state in South America are spatially aggregated towards
342   the border between Brazil, Colombia, and Peru – covering a considerable portion of the Central Amazon (Fig.
343   3). Whereas for Africa, these forests exist in moderate to small patches towards the northern and southern
344   extent of central Congo rainforests. We observe that these transitions account for most of the projected
345   changes to forests' states across both continents (Fig. 2d,e), with the transition to just the 'highly water-limited
346   forest' accounting for more than three-fourths of all such transitions (Fig. 3). We observe that South American
347   forests gradually become increasingly water-limited under warmer climates, with maximum and minimum
348   projected transition of 1.89×10^6 km^2 (23.4%) and 1.61×10^6 km^2 (19.9%) observed under the highest and lowest
349   emission scenarios, respectively (Fig. 2d,e). Whereas for Africa, the change in the water-limited state of the
350   forests under different SSP scenarios remains almost similar (i.e., median 1.14 ($\pm$0.06) $\times 10^6$ km^2; 19.6-22.2%).
351   Analysis of their hydroclimatic changes reveals that water-limitation is induced by both a decrease in
352   precipitation and an increase in seasonality in South America (Fig. S13). In contrast, water-limitation in Africa is
353   driven solely by an increase in seasonality. We observe that these newly water-limited forests seem to have
354   permeated to regions that were previously (under the current climate) dominated by lowly and moderately
355   water-limited forests (Fig. 3). Here, this shift only signifies the changes to hydroclimatic conditions allowing
356   forests to transition to a more water-limited state, rather than the changes to the floristic composition of
357   terrestrial species from one location to another. Although such a shift under changing climate is not unlikely
358   (Esquivel-Muelbert et al., 2019), they are not analysed in this study.

359   Forests that revert to a 'less' water-limited state in South America are primarily observed in the south-
360   eastern Amazon, with small patches observed towards eastern Brazil and the western coast of Equatorial
361   Guinea and Gabon (Fig. 3). For Africa, the reverted forests exist in patches in the northern and southern regions
362   of the Congo rainforest. Furthermore, for South America, we observe a gradual decrease in these reversions

11

363 with an increase in warming. Here, we observe the lowest reversion of 0.23×10^6 km^2 (2.8%) under the highest

364 emission scenario and the highest reversion of 0.67×10^6 km^2 (8.4%) under the lowest emission scenario (Fig.

365 2f,g). For Africa, these trends remain almost similar under all SSPs (i.e., median 0.18 (±0.05) × 10^6 km^2; 2.2-

366 3.5%). Comparing these transitions with their hydroclimatic changes reveals an overall increase in precipitation

367 (Fig. S14). Interestingly, we observe a much higher precipitation increase for South America under high-

368 emission scenarios than those in lower-emission scenarios. However, we find that precipitation seasonality is

369 also higher for these ecosystems under warmer climates (Fig. S14). This suggests that increased precipitation

370 without changes to precipitation seasonality helps decrease the water-limitation of the ecosystem, compared

371 to the ecosystems that experienced a simultaneous increase in both.

372 Our sensitivity analysis, detailed in Appendix B1, reveals a consistent pattern of forest transitions across
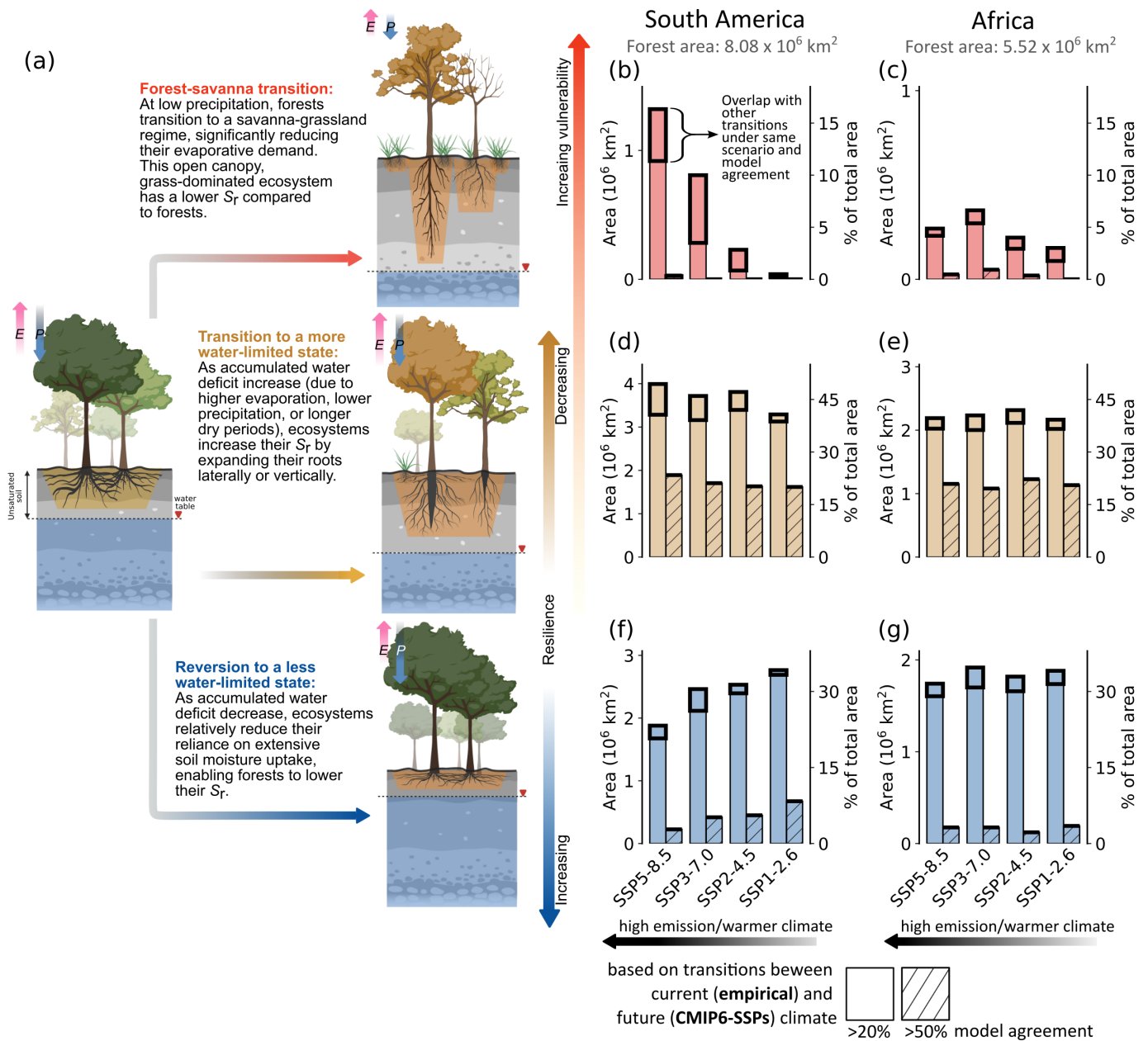
373 various scenarios.

374

375

376

377

378

Figure 2: Comparing the potential transitions under different SSP scenarios. (a) The state of the ecosystem, both above- and below-ground, (post-transition) under future climate, quantifying **(b,c)** forest-savanna transition, **(d,e)** forests' that transition to a more water-limited state and **(f,g)** revert to a less water-limited state for South America and Africa (present forest area mentioned on the top of (b,c)), respectively. For the analysis above, transitions are calculated for grid cells with model agreement >20% (plain bar plot) and >50% (hatched bar plot). These quantifications show changes in the forest area based on ecosystem transitions under empirical-current (2001-2012) and future (2086-2100) climate conditions. For all these transitions, we assume that the hydroclimate and vegetation are in equilibrium. Analyses comparing ecosystem transitions based on CMIP6-historical (2000-2014) and future (2086-2100) climate conditions are shown in Fig. S10 and S11. For each transition, the total area of spatial overlap with other transitions under the same SSP scenario and model agreement is highlighted with thick black bars. The *P* and *E* arrows in (a) describe the relative magnitude of precipitation and evaporation fluxes. The illustration in (a) is adapted from Singh et al. (2020) and created with BioRender.com.
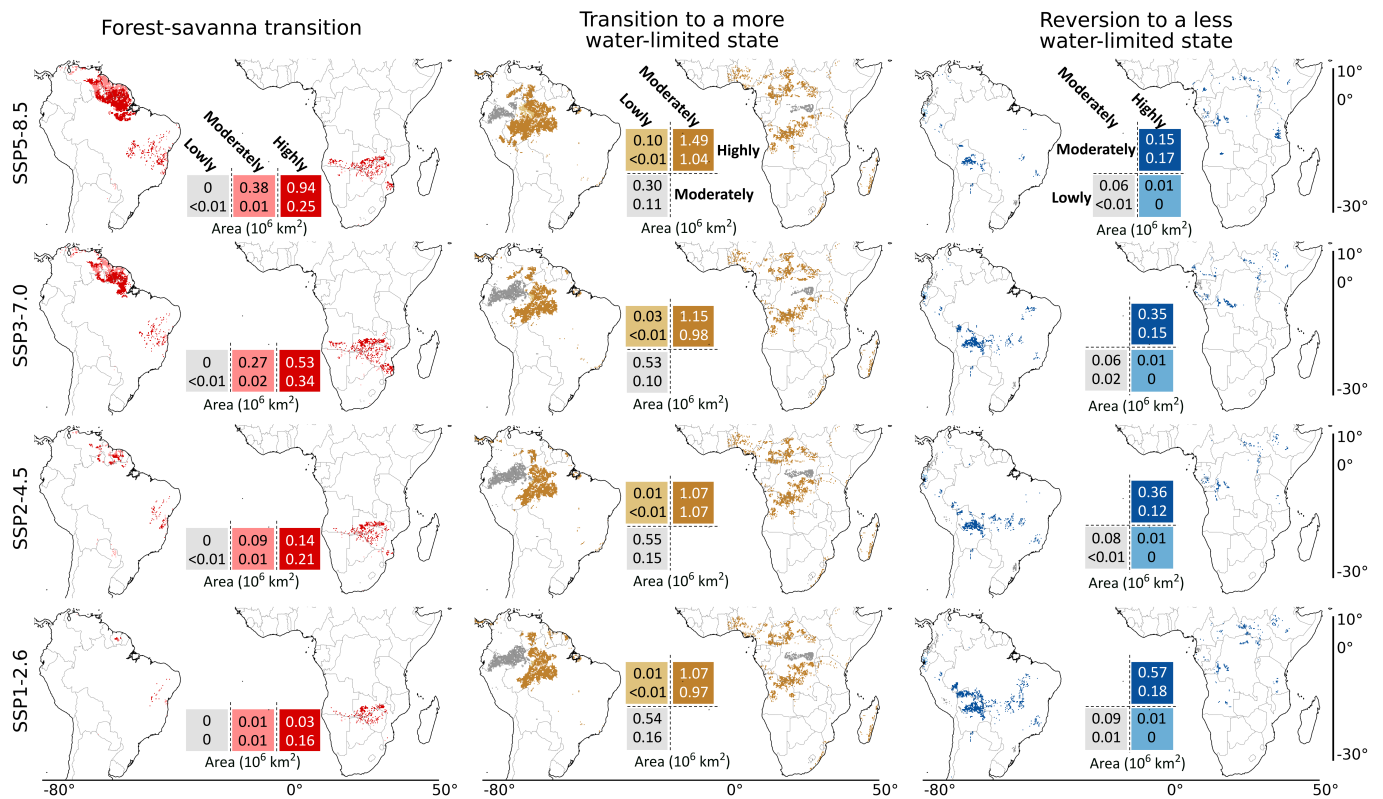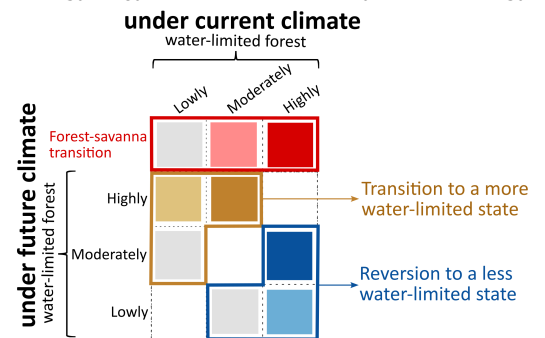
Figure 3: Spatial extent of potential transitions with respect to their current state under different SSP scenarios. We analysed transitions, explicitly focusing on forest-savanna transition, transition to a more water-limited state, and reversion to a less water-limited state, by comparing different ecosystem classes under current (empirical; 2001-2012) and future (SSPs; 2086-2100) climate conditions (as defined in Fig. 2). All transitions shown above are analysed for moderate-high (>50%) model agreement, except forest-savanna transition, for which moderate (>20%) model agreement is considered. Values overlaying the legends correspond to the total area of transition for South America (top values) and Africa (bottom values).

4   Discussion

4.1   Asynchronous resilience risks under future climate change

Our analysis reveals the spatial extent of potential ecosystem transitions in South America and Africa and their vulnerability to future climate change (Fig. 2 and 4). For South America, we find a clear indication of a decrease in forest resilience (i.e., an increase in water-limited forests) and an increase in forest-savanna transition risk under warmer climates (Fig. 2b,d,f). In contrast, these trends are not symmetric for Africa, where transition risk

14

shows only slight variation across the different SSPs (Fig. 2c,e,g). Similar to the results of this study, previous studies on rainforest tipping have also suggested that exceeding 1.5-2°C will considerably increase the tipping risk (Flores et al., 2024; Jones et al., 2009; Parry et al., 2022), with the Guyana Shield in the Amazon being the most susceptible under future climate change (Cox et al., 2004; Staal et al., 2020) (Fig. 3 and Table S3). Previous studies also agree that, in contrast to the Amazon, the projected risk to Congo rainforests is not substantial (Higgins and Scheiter, 2012; Staal et al., 2020) (Fig. 2). Despite it being unclear to what extent the ESMs represent the correct carbon-water dynamics (Koch et al., 2021), our results show a further divergence between Amazon's and Congo's responses to different SSPs (Fig. 2 and Fig. S12-S14). This could either be caused simply by a different response to changes in precipitation patterns over the respective regions (Kooperman et al., 2018; Li et al., 2022) or a different response to increased CO_2 levels in the atmosphere (Brienen et al., 2015; Hubau et al., 2020; Trumbore et al., 2015).

Previous empirical studies have linked these divergent responses to evolutionary and biogeographical differences between the ecosystems, which resulted in distinct species pools that uniquely influence each ecosystem's adaptability and response to climate change (Fleischer et al., 2019; Hahm et al., 2019; Hubau et al., 2020; Slik et al., 2018). These studies found that forest ecosystems in the Amazon tend to be more dynamic – grow faster due to high CO_2 levels in the atmosphere – than those in the Congo rainforests. However, these fast-growing trees also die young due to them investing substantially less in their adaptive strategies against perturbations than (less dynamic) old-growth forests (Brienen et al., 2015; Körner, 2017; Rammig, 2020). This makes the Amazon rainforest especially sensitive to CO_2 emissions pathways, as the positive influence of CO_2 fertilisation-induced growth is counteracted by the negative impact of warming and droughts, thereby exacerbating the risk of forest mortality under high emission scenarios (Brienen et al., 2015; Hubau et al., 2020; Yang et al., 2018). In this case, the projected changes to the future hydroclimate could be an artefact of decreased transpiration and precipitation due to forest mortality, rendering the rainforests vulnerable to tipping. In contrast, terrestrial species in Congo rainforests appear more resilient, having adapted to severe droughts during glacial periods, which makes them better equipped to handle episodic water-induced perturbations than Amazon (Cole et al., 2014).

Nevertheless, with compounding influence from land-use and climate-induced hydroclimatic changes (Davidson et al., 2012), these rainforests risk tipping to a savanna state. Our results highlight that by keeping the mean global surface temperature below 1.5-2°C warming (which in this case is equivalent to SSP1-2.6 relative to the pre-industrial), we minimise forest-savanna transition risk and maximise recovery – thereby improving the resilience of rainforest ecosystems (Fig. 2, 3 and 4).

4.2   Changes in atmospheric moisture flow drives forest-savanna transition

Among all transitions, the most noticeable and catastrophic (since it is difficult to revert) is the forest-savanna transition projected in the Amazon's Guiana Shield of South America, and over the southern and south-eastern parts of Africa (Fig. 3 and 4). These transitions are associated with the shifting of the inter-tropical convergence zone (ITCZ) (Mamalakis et al., 2021), which decreases precipitation and increases precipitation seasonality over the continents. For South America, the creation of these low-pressure bands allows the trade winds to bring in considerable moisture from the equatorial Atlantic Ocean over to Amazon by passing through the Guiana Shield and ultimately carrying it across the La Plata Basin via the South American low-level jet (Bovolo et al., 2018; van der Ent et al., 2010; Zemp et al., 2014). Similarly, for Africa, south-eastern trade winds bring moisture from the Indian Ocean over the centre of the African continent (Mamalakis et al., 2021).

Under a warmer climate, sea surface temperature over the equatorial Atlantic and the northern Indian Ocean is projected to increase (Pascale et al., 2019; Zilli et al., 2019), leading to a southward shift in ITCZ over the eastern Pacific and Atlantic Oceans, and northward over east Africa and the Indian Ocean (Mamalakis et al., 2021; Xie et al., 2010). Previous studies also acknowledge that the intense surface warming over the Sahara under future climate can also attract ITCZ northwards in Africa (Cook and Vizy, 2012; Dunning et al., 2018; Mamalakis et al., 2021). Since these shifts in ITCZ can potentially both mitigate and aggravate (especially critical for highly water-limited forests) the impact of (accumulated) water-deficit on the forest ecosystem, including those caused by localised deforestation (Leite-Filho et al., 2021; Schumacher et al., 2022; Staal et al., 2018; Wunderling et al., 2022); it warrants the need to include changes in atmospheric circulation for studies analysing the impact of future climate on the resilience of forest ecosystems (Staal et al., 2020; Zemp et al., 2017).
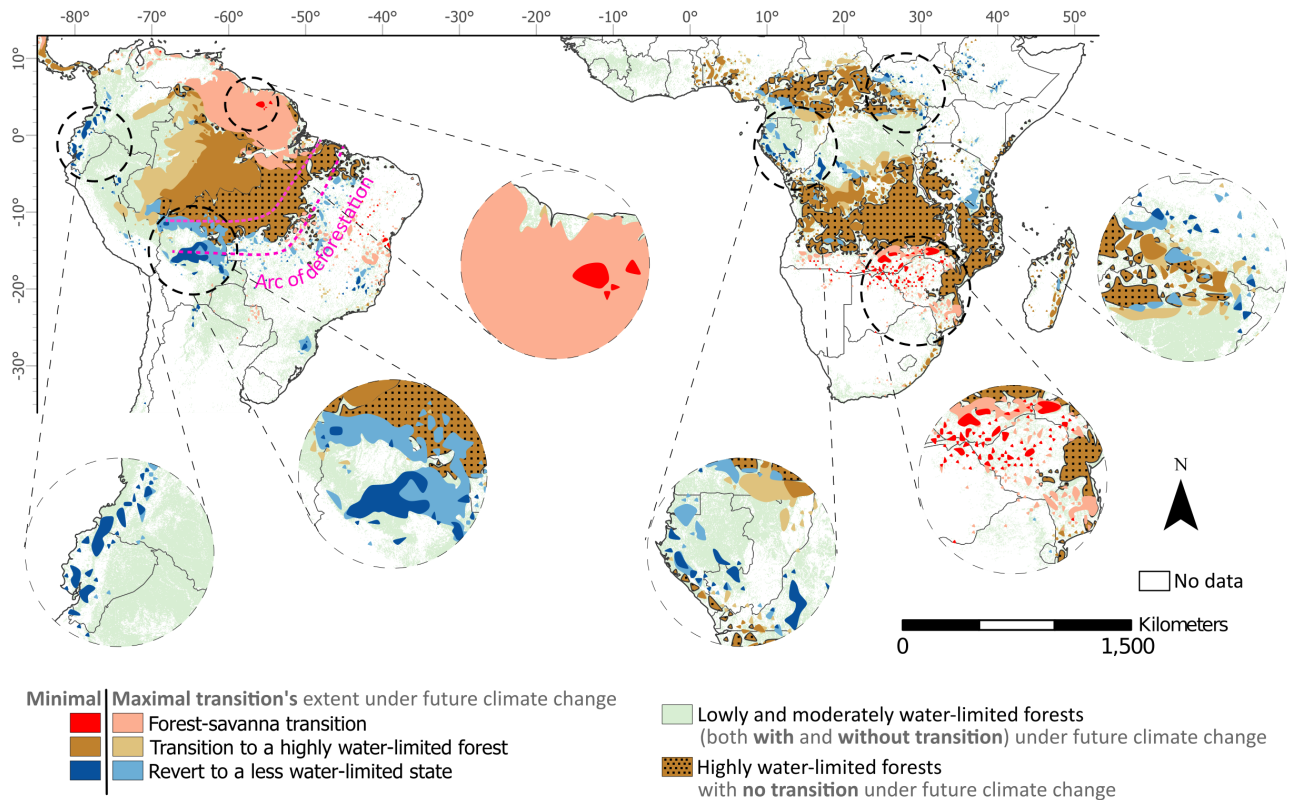
Figure 4: Minimal and maximal extent of potential ecosystem transitions under future climate change in the entire study region over South America and Africa. The three transition types are: forest-savanna transition, from any class to highly water-limited forests, and to a less water-limited state (see definitions in Fig. 2 and 3). For better visualisation of these transitions, in this figure, we first converted all grid cells to shape, merged them, and then smoothed them using the 'polynomial approximation with exponential kernel' function (with a tolerance value of 1) in ArcGIS pro. The unsmoothed version of the transitions is shown in Fig. 3. The minimal and maximal represent the minimum and maximum possible extent of transitions (as quantified in Fig. 3) based on changes between current (empirical; 2001-2012) and future (SSPs; 2086-2100) climate conditions regardless of the SSP scenarios.

### 4.3   Discrepancy between prescribed future land-use and projected transitions

The land-use information in CMIP6-ESMs is not biophysically simulated, but prescribed based on simulations from Integrated Assessment Models (IAMs) for each SSP scenario (Hurtt et al., 2020). Therefore, it is valuable to examine whether these prescribed land-use scenarios agree or conflict with the changes projected (assuming equilibrium between hydroclimate and the ecosystem) by our S_r-based ecosystem transitions (Fig. 5 and Fig. S15-S17).

The most noticeable discrepancies are observed in South America, where the extent of forest-savanna transitions is underestimated in prescribed land-use scenarios compared to those projected in this study (i.e., prescribed land-use predicts forests in the region whose hydroclimate can't support forest; Fig. 4 and 5a). Additionally, in South America, our analysis highlights the potential of some forests reverting to a 'less water-limited state' in places where the prescribed land-use in the ESMs suggest non-forest landscape (Fig. 4 and 5c).

484 These discrepancies arise because the prescribed land-use in CMIP6-ESMs do not shift in response to
485 hydroclimatic changes. Despite our approach assuming equilibrium and overlooking the temporal dynamics of
486 transitions, based on broad climate change pattern (Sect 4.2), we believe it more accurately represents the
487 ecohydrological state of the ecosystems.

488   However, these prescribed land-uses can introduce errors in subsequent biophysical processes
489 simulated in ESMs (Ma et al., 2020), affecting the accuracy of projected transitions. For example, prescribing a
490 region as a forest that would be grassland in the future will lead to the extraction of deeper subsoil moisture in
491 ESMs, which (actual) grasslands do not have the capacity to access (Ahlström et al., 2017; Yu et al., 2022). This
492 will result in an overestimation of the ecosystem's evaporation, potentially altering precipitation patterns
493 downwind and leading to inaccurate water budget assessments for these ecosystems. Consequently, causing
494 erroneous projections of the ecosystem state. These discrepancies underscore the urgent need for
495 enhancements in the land surface components of ESMs, enabling dynamic simulations of vegetation-climate
496 feedbacks. Such improvements would provide a more accurate representation of the ecohydrology of
497 terrestrial ecosystems and their response to changing climate conditions.

498
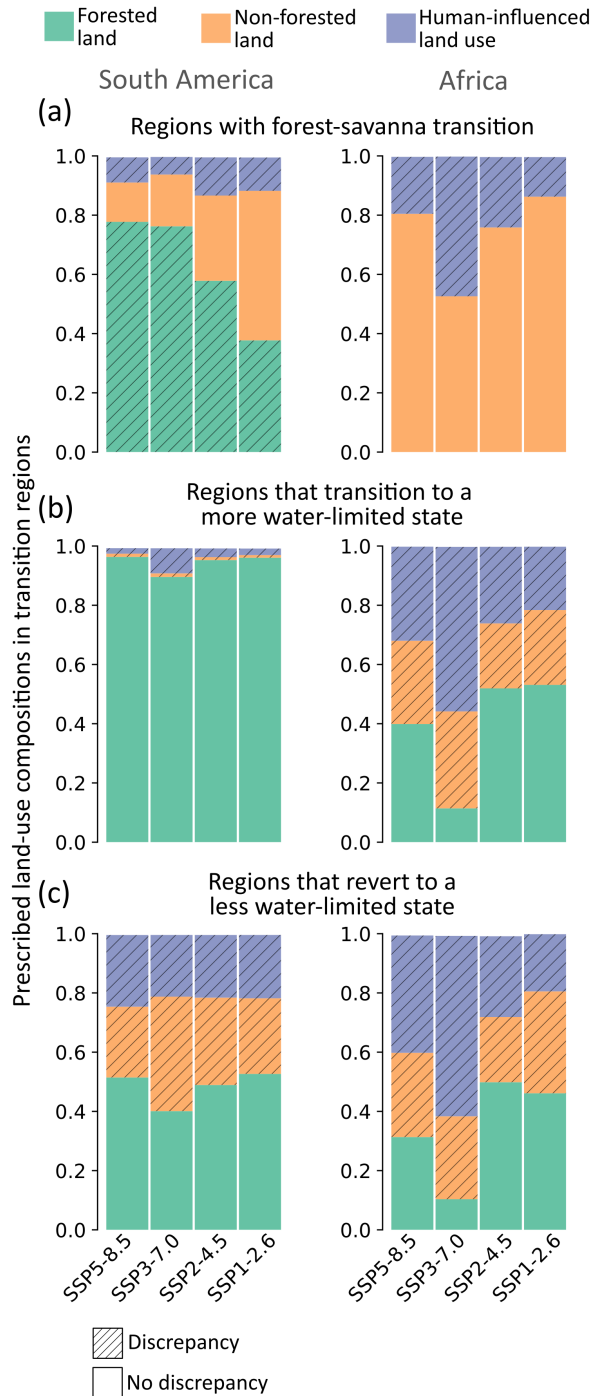
Figure 5: Prescribed land-use composition for each transition region under different SSP scenarios (median 2086-2100), calculated as the ratio between the prescribed land use area and the projected transition area. Regions where IAM prescribed land use are same as the projected transitions (from Fig. 3) are shown in plain colours (i.e., no discrepancy). Whereas regions where IAM-prescribed land use differs from projected transitions are hatched (i.e., discrepancy).

4.4   Limitations

This study assumes that the S_r-derived thresholds used to classify terrestrial ecosystems under current climate conditions remain valid under future climate change. However, forests themselves are dynamically adapting

their structure and functions in response to climate change, altering their critical thresholds (Doughty et al., 2023). Thus, assuming a static critical threshold may lead to inaccuracies in estimating forests' resilience to future climate change. For instance, under the CO_2 fertilisation effect, forests may become more water-use efficient (i.e., transpire less and therefore need for a lower S_r) (Xue et al., 2015), potentially delaying their tipping under warming scenarios compared to those projected in this study. Conversely, factors such as nutrient limitation (Condit et al., 2013) or extensive human influence (van Nes et al., 2016) in the ecosystem might lead to an earlier tipping than anticipated.

However, the uncertainty surrounding the effect of CO_2 fertilisation, nutrient limitation, and human influence on vegetation remain significant research frontiers for enhancing our understanding of rainforest tipping under future climate change (Fleischer et al., 2019; Hofhansl et al., 2016). Additionally, factors such as precipitation variability, species composition, soil properties, and topography can contribute to varied local-scale forest responses to future climate change (Staal et al., 2020). It should also be noted that though these uncertainties may hinder our understanding of local-scale forest resilience, the influence of future hydroclimatic changes on forests still constitutes major prediction uncertainties. Therefore, in this study, regardless of how these influences are parametrised or simulated in each ESM, we assume that hydroclimatic estimates projected by the ESMs represent the actual climate.

Of course, this assumption opens us and other studies projecting forest conditions to future climate change to certain limitations. Our ability to project forest-savanna transitions (or any transition) relies on the model's capacity to simulate complex feedbacks. Some models capture complex vegetation-atmosphere interaction, simulating local and regional scale feedbacks across time (Ferreira et al., 2011; Jach et al., 2020); others reply on simpler parametrisation (Nof, 2008) (e.g., parametrisation of CO_2 fertilisation; Koch et al., 2021). However, caution should be taken to not overgeneralise the functioning of tropical forests just from the analysis presented in this study, and also realise the current potential of ESMs to simulate them (Staal et al., 2020). We believe that by considering simulations from multiple ESMs under different SSP scenarios, not only do we highlight the agreements and conflicts between potential transitions; but also allow future studies to disentangle vegetation-climate feedbacks and improve the modelling of local-scale interactions (e.g., vegetation's water-uptake profile, species response to CO_2 fertilisation) in the ESMs.

5 Conclusions

Classifying terrestrial ecosystems based on empirical and CMIP6 ESMs-derived S_r allowed us to assess the future transitions in the rainforest ecosystems. Our findings indicate that climate under the lowest emission scenarios significantly reduces the risk of rainforest tipping and maximises reversion to a less water-limited state, while climate under the high emission scenarios have the opposite effect on the forest ecosystem. Specifically, in the

Amazon rainforest, the risk of forest-to-savanna transition increases considerably with incremental increase in warming. Conversely, in the Congo, the variation in transition risk across different emission scenarios is relatively minor.

Notably, our analysis suggests very limited tipping risk that is 'unavoidable' (i.e., regions prone to a forest-savanna transition in all scenarios), and the vast majority of potential transition risks can still be avoided by steering towards a less severe climate scenario, thereby underscoring the critical window of opportunity. Moreover, regions projected to revert to a less water-limited state could potentially become more amenable to restoration and responsive to deforestation prevention efforts. This study highlights the importance of restricting global temperature change below 1.5-2°C warming relative to the pre-industrial levels to prevent forest tipping risks and provide the best conditions for effective ecosystem stewardship.

Appendix A: Methodology

A1. Root zone storage capacity calculation

Our method to calculate S_r is adopted from Singh et al. (2020). For estimating S_r, we first obtained the water deficit (D_t) at daily time step from the daily estimates of precipitation (P_t) and evaporation (E_t) (Fig. A1) using:

$$D_t = E_t - P_t \tag{A1}$$

Here, t denotes the day count since the start of the simulation, with simulation for each grid starting in the month with maximum precipitation. Second, we calculated the accumulated water deficit integrated at each one-day timestep for one year using:

$$D_{a(t+1)} = \max\{0, D_{a(t)} + D_{t+1}\} \tag{A2}$$

Where $D_{a(t+1)}$ is the accumulated water deficit at each time step (Fig. A1). Here, an increase in the accumulated water deficit will occur when $E_t > P_t$, and a decrease when $E_t < P_t$. However, since this algorithm estimates a running estimate of root zone storage reservoir size, we use a maximum function to calculate the accumulated water deficit, which by definition can never be below zero. Not allowing $D_{a(t+1)}$ to be negative also means that excess moisture from precipitation will either contribute to deep drainage or runoff. Lastly, the maximum accumulated annual water deficit ($D_{a,y}$) will represent the maximum storage required by the vegetation to respond to the critical dry periods (Fig. A1).

$$D_{a,y} = \max\{D_{a(t+1)}\} \quad t = 1:n-1 \tag{A3}$$

This simulation runs for a whole year, with n denoting the number of days in year y.

571   Although different terrestrial ecosystems (e.g., forest, savanna and grasslands) adapt to different

572   drought return periods (de Boer-Euser et al., 2016; Gao et al., 2014; Wang-Erlandsson et al., 2016). For instance,

573   grasslands and savanna adapt to shorter drought return periods (i.e., <10 years and 10-20 years, respectively).

574   In contrast, forests adapt to long drought return periods (>40 years) (Wang-Erlandsson et al., 2016). For this

575   study, we use a uniform 20-year drought return period (following Bouaziz et al., 2020; Nijzink et al., 2016) to

576   avoid any artificially introduced transitions between different ecosystems. Thus, this 20-year drought return

577   period S_r refers to the maximum amount of root zone moisture accessible to vegetation for transpiration during

578   the largest accumulated annual water deficit expected every twenty years under static climate conditions. This

579   we analyse using on the Gumbel extreme value distribution (Gumbel, 1958) and apply it to normalise all $\overline{D_{a,y}}$.

580   The Gumbel distribution ($F(x)$) is given by:

$$F(x) = \exp\left[-\exp\left[-\frac{(x-\mu)}{\alpha}\right]\right] \tag{A4}$$

582   Where μ and α are the location and scale parameters, respectively. We calculate this using the python
583   package 'skextremes'(skextremes Documentation):

$$S_r = \overline{D_{a,y}} + K \times \sigma_{n-1} \tag{A5}$$

585   Where K is the frequency factor given by:

$$K = \frac{y_t - y_n}{S_n} \tag{A6}$$

587   And y_t is the reduced variate given by:

$$y_t = -\left[\ln\left[\ln\left(\frac{T}{T-1}\right)\right]\right] \tag{A7}$$

589   Where T is the drought return period (i.e., 20 years used in this study), $\overline{D_{a,y}}$ is the mean annual

590   accumulated deficit for the years 2001-2012, σ_{n-1} is the standard deviation of the sample. Also, y_n is the

591   reduced mean and S_n is the reduced standard deviation, which for n = 11 years (since we are calculating S_r in a

592   hydrological year – simulation starts mid-year – we therefore lose one year) is equal to 0.4996 and 0.9676,

593   respectively (Gumbel, 1958).

594   Since the CMIP6 (-historical and -SSP estimates, the timeframe considered are 2000-2014 and 2086-

595   2100, respectively) doesn't have daily estimates of evaporation and precipitation for all Earth System Models

596   (ESMs), we directly use the monthly estimates of precipitation and evaporation to modify Eq. (A1) as:

$$D_t = E_{t(monthly)} - P_{t(monthly)} \tag{A8}$$

Here, *t(monthly)* denotes the month count since the start of the simulation. The rest of the steps (Eq. A2-A7) remain the same for CMIP6 datasets. For CMIP6 runs, y_n and S_n in Eq. (6) are calculated for *n* = 14 years (Eq. A7) equal to 0.5100 and 1.0095, respectively. The S_r estimates derived from daily and monthly empirical estimates (from Eq. A1 and A8) are compared in Fig. S8 to evaluate uncertainty.
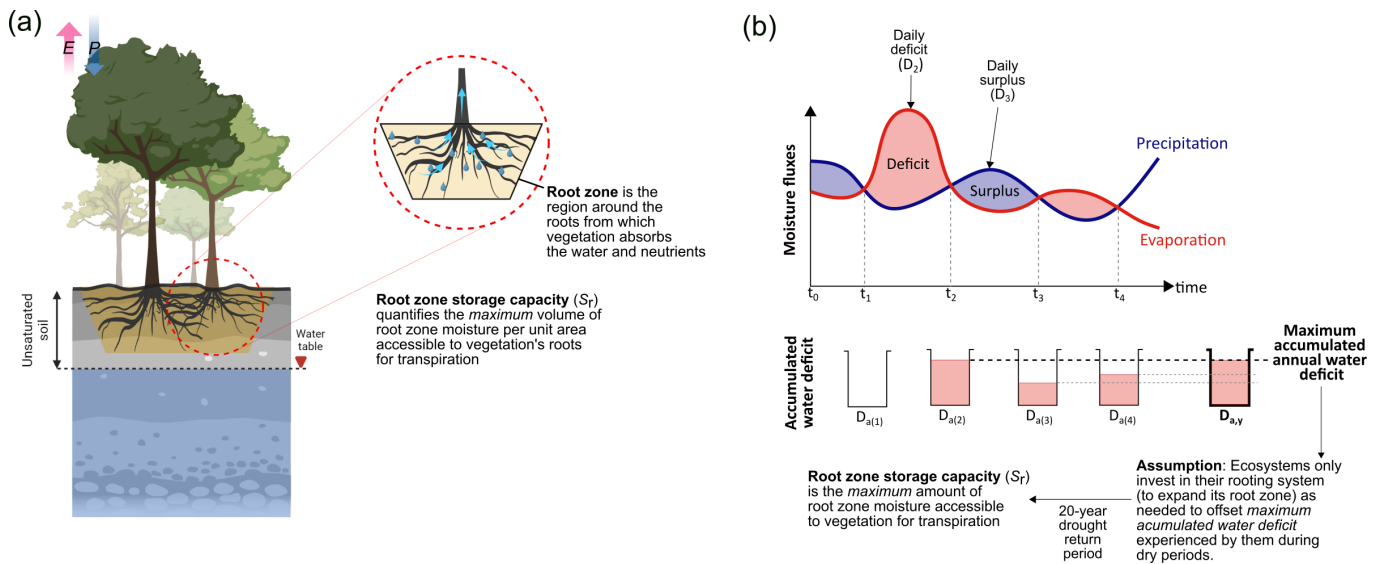
Figure A1: The figure illustrates the root zone storage capacity (S_r) of the ecosystem. (a) We show the difference between the ecosystem's root zone and how that constitutes its S_r. (b) Conceptual illustration of how the ecosystem's precipitation and evaporation fluxes constitute the maximum accumulated annual water deficit ($D_{a,y}$) and S_r. The figure is adopted from Singh (2023) and Wang-Erlandsson et al. (2016).

**A2. Abiotic and biotic factors influence soil moisture availability**

In this study, S_r quantifies the hydrological buffer necessary for an ecosystem to maintain its structure and functions, reflecting the amount of root zone soil moisture available to vegetation for transpiration. Our mass-balance-based S_r methodology, while not directly distinguishing between the biotic and abiotic influences on soil moisture and root characteristics, does incorporate their critical role in shaping the ecohydrology of the ecosystem under climate change. By utilising empirical precipitation and evaporation data, our approach theoretically captures the combined impact of these biotic and abiotic factors on the actual hydrological regime (including soil moisture) of the ecosystem (Sect. 2.3.2).

We acknowledge that abiotic factors such as soil texture, structure, and depth profoundly affect soil water-holding capacity (Fayos, 1997). For instance, field studies suggest that clay and organic-rich soils exhibit superior water retention capabilities due to their fine textures and high surface areas, which is crucial to vegetation for moisture uptake during extended dry periods (Bronick and Lal, 2005; Fayos, 1997). Additionally,

the depth and porosity of soil also dictate its ability to absorb and store water in the soil, with deeper, less compacted soils providing a higher buffer against drought by allowing greater water infiltration (Indoria et al., 2020; Smith et al., 2001). Climate change, by altering temperature and precipitation patterns, can modify these abiotic soil properties, potentially leading to loss in soil water retention capacity through erosion and compaction (Dexter, 2004).

Moreover, biotic factors, including plant-root dynamics and microbial activity, also play essential roles in shaping the ecosystem (Brunner et al., 2015; Sveen et al., 2024). Deep and extensive root systems not only directly improve access to deeper soil moisture, but also physically modify the soil to enhance its permeability and storage (Canadell et al., 1996; Jackson et al., 1996). Additionally, microbial processes contribute by breaking down organic matter, thereby improving the soil's structural integrity and ability to retain water (Dittert et al., 2006). These biotic interactions, coupled with changing abiotic factors under climate change, underscore the complex dynamics that govern soil moisture availability and ecosystem resilience. However, this study does not consider the direct impact of future climate change on biotic and abiotic factors, nor their influence on ecosystems, beyond changes to S_r.
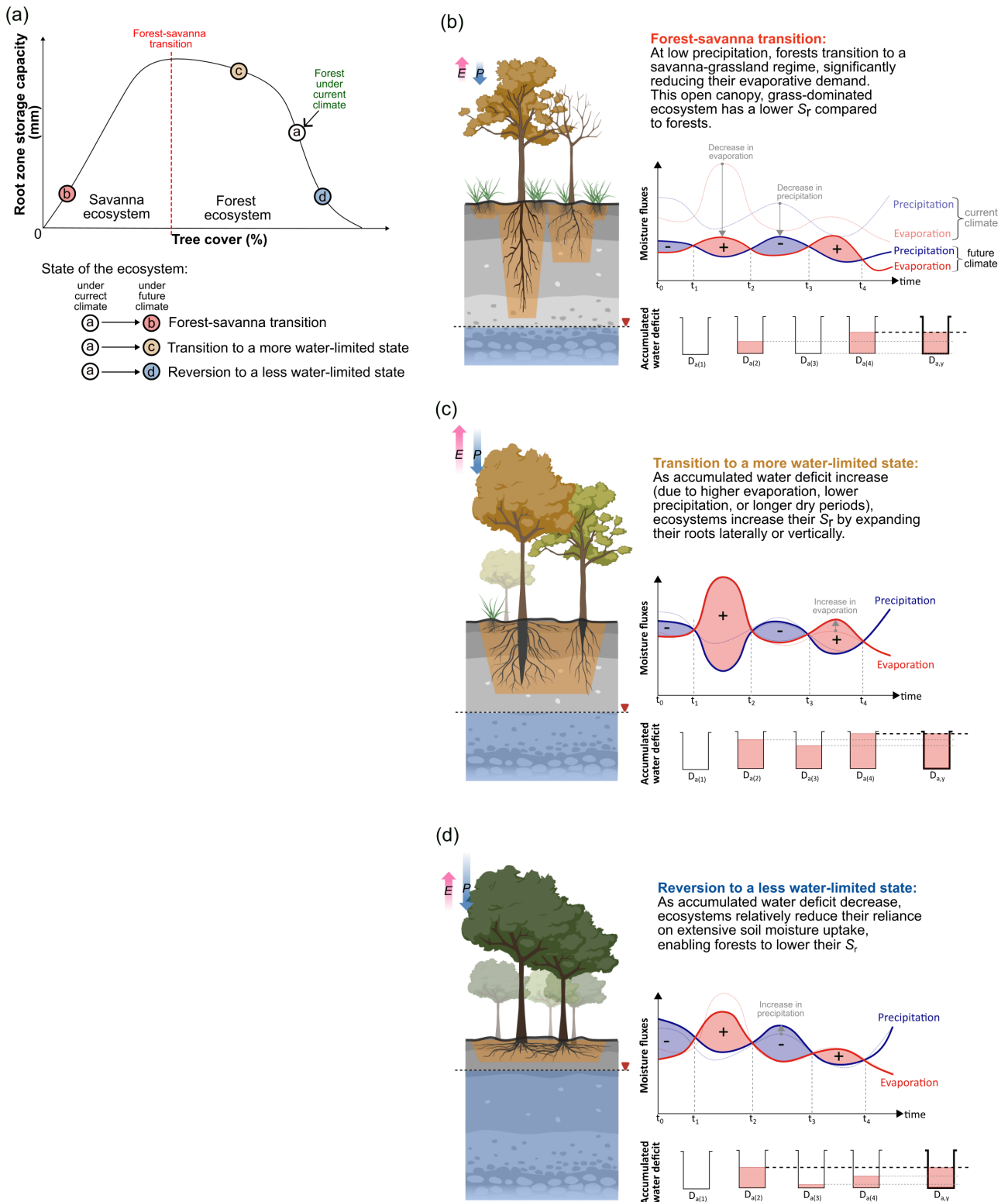
Figure A2: (a) The figure compares the root zone storage capacity (S_r) with the ecosystem state (i.e., tree cover). This figure expands on the conceptual illustration from Fig. A1, showing how the ecosystem's precipitation and evaporation fluxes contribute to S_r under different forest transition scenarios: (b) forest-savanna transition, (c) transition to a more water-limited state, and (d) reversion to a less water-limited state.

A3. Using precipitation to discern savanna from forests under future climate change

Under future climate change, some ecosystems will remain forest, while others may transition to savanna. In our S_r-based framework, without information about above-ground forest structure, it is difficult to discern whether an ecosystem is a forest or savanna just with S_r (for instance, an ecosystem with S_r of 200 mm can either be a moderately water-limited forest or savanna; Sect. 2.3.2). Differentiating these ecosystems is easier under the current climate, where we have several remote sensing products capturing vegetation structure (e.g., tree cover density, tree height, floristic patterns) (Aleman et al., 2020; Hirota et al., 2011; Xu et al., 2016). However, under future climate, we must find a proxy, since land-use information in ESMs are prescribed (i.e., not biophysically simulated) (Ma et al., 2020).

To address this, previous studies have either relied on vegetation structure proxies provided by ESMs (e.g., net primary productivity) (Boulton et al., 2013; Jones et al., 2009), or assumed that terrestrial ecosystems are in equilibrium with their climate (Staal et al., 2020) (see Supplement). In this study, we adopted the latter approach and utilised climate variables, specifically (bias-corrected) mean annual precipitation and the precipitation seasonality index, as proxies to make this distinction (Fig. S4). The climate conditions (or range) necessary for forest ecosystems to sustain themselves are determined by comparing empirical estimates of mean annual precipitation and precipitation seasonality index with S_r. These estimates are then bias-corrected (following the same methods described in Sect. 2.3.3) before applying them to future climate scenarios. This (revised) classification of terrestrial ecosystems is then used to assess forest transitions under future climate change scenarios.

Appendix B: Results

B1. Sensitivity analysis reveals robust performance of the framework

Sensitivity analysis reveals that by setting an extreme S_r threshold – signifying a forest-savanna transition for ecosystems that cannot maintain their above-ground structure at high S_r – we observe some shifts near the already projected risk regions and coastal areas (Fig. 3 and Fig. S18). However, the transition risk identified in the coastal regions may be an artefact of interpolating hydroclimate estimates to higher resolution Additionally, since evaporation is more prevalent over oceans than land, this could result in high S_r values, thereby projecting an elevated tipping risk in these coastal areas.

We also discover that variations in the evaporation datasets and return periods used for calculating S_r have minimal effect on forest transitions (Fig. S19 and S20). Although the forest classification thresholds may shift with different evaporation products under current climate conditions (Singh et al., 2020), our histogram equivalence method ensures that forest classifications under future climates adjust accordingly, resulting in only minor alterations to the final outcome (Fig. 1b and Fig. S19). Furthermore, while S_r values tend to increase

673   with increase with shorter return periods, the impact of these changes becomes less significant with longer

674   return periods (Wang-Erlandsson et al., 2016); leading to minor variations in the end results (Fig. S20).

675   Moreover, lowering the forest-savanna transition thresholds can reduce the risk of forest-savanna

676   transition since it expands the associated range of climate conditions (i.e., mean annual precipitation and

677   seasonality) necessary for forests to sustain their structure and functions (Fig. S21). Conversely, increasing the

678   forest-savanna transition threshold leads to an opposite trend, where the risk of transition increases (Fig. S22).

679   Despite these sensitivity analyses, the variation in transition magnitudes is minor, and the trends across

680   different SSP scenarios for both continents remain consistent (Fig. 2 and Fig. S18-S22). Therefore, the

681   conclusions drawn from this study remain robust, even with variations in factors that could potentially affect

682   forest transitions.

Data availability

All the data generated during this study is made publicly available at Zenodo:
https://zenodo.org/record/7706640. Other datasets that support the findings of this study are publicly available at: (CMIP6; citations referred to in Table S2) https://aims2.llnl.gov/, (Root zone storage capacity; empirical) https://github.com/chandrakant6492/Drought-coping-strategy, (P-CHIRPS) https://data.chc.ucsb.edu/products/CHIRPS-2.0/, (E-BESS) ftp://147.46.64.183/, (E-FLUXCOM) ftp.bgc-jena.mpg.de, (E-PML) https://data.csiro.au/collections/#collection/CIcsiro:17375v2, (E-ERA5) https://cds.climate.copernicus.eu/cdsapp#!/dataset/reanalysis-era5-single-levels, (Globcover) http://due.esrin.esa.int/page_globcover.php. Potential transitions for each ESM based on the comparison between empirical (2001-2012) and SSP (2086-2100) scenarios are presented in the Supplement.

Code availability

The python-language scripts used for the analyses presented in this study are available from GitHub: https://github.com/chandrakant6492/Future-forest-transitions-CMIP6. The python-language code for calculating (empirical) root zone storage capacity is available from GitHub:
https://github.com/chandrakant6492/Drought-coping-strategy.

Acknowledgements

Author contributions

All authors contributed to the conceptualisation of this research. CS performed the analyses and wrote the initial draft. All authors contributed to the discussion and revisions, leading to the final version of the manuscript.

Competing interests

The authors declare no competing interests.

References

Ahlström, A., Canadell, J. G., Schurgers, G., Wu, M., Berry, J. A., Guan, K., and Jackson, R. B.: Hydrologic resilience and Amazon productivity, Nature Communications, 8, 387, https://doi.org/10.1038/s41467-017-00306-z, 2017.

Albasha, R., Mailhol, J.-C., and Cheviron, B.: Compensatory uptake functions in empirical macroscopic root water uptake models – Experimental and numerical analysis, Agricultural Water Management, 155, 22–39, https://doi.org/10.1016/j.agwat.2015.03.010, 2015.

Aleman, J. C., Fayolle, A., Favier, C., Staver, A. C., Dexter, K. G., Ryan, C. M., Azihou, A. F., Bauman, D., Beest, M. te, Chidumayo, E. N., Comiskey, J. A., Cromsigt, J. P. G. M., Dessard, H., Doucet, J.-L., Finckh, M., Gillet, J.-F., Gourlet-Fleury, S., Hempson, G. P., Holdo, R. M., Kirunda, B., Kouame, F. N., Mahy, G., Gonçalves, F. M. P., McNicol, I., Quintano, P. N., Plumptre, A. J., Pritchard, R. C., Revermann, R., Schmitt, C. B., Swemmer, A. M., Talila, H., Woollen, E., and Swaine, M. D.: Floristic evidence for alternative biome states in tropical Africa, PNAS, 117, 28183–28190, https://doi.org/10.1073/pnas.2011515117, 2020.

Armstrong McKay, D. I., Staal, A., Abrams, J. F., Winkelmann, R., Sakschewski, B., Loriani, S., Fetzer, I., Cornell, S. E., Rockström, J., and Lenton, T. M.: Exceeding 1.5°C global warming could trigger multiple climate tipping points, Science, 377, eabn7950, https://doi.org/10.1126/science.abn7950, 2022.

Arora, V. K., Seiler, C., Wang, L., and Kou-Giesbrecht, S.: Towards an ensemble-based evaluation of land surface models in light of uncertain forcings and observations, Biogeosciences, 20, 1313–1355, https://doi.org/10.5194/bg-20-1313-2023, 2023.

Baker, J. C. A., Garcia-Carreras, L., Buermann, W., Souza, D. C. de, Marsham, J. H., Kubota, P. Y., Gloor, M., Coelho, C. A. S., and Spracklen, D. V.: Robust Amazon precipitation projections in climate models that capture realistic land–atmosphere interactions, Environ. Res. Lett., 16, 074002, https://doi.org/10.1088/1748-9326/abfb2e, 2021.

Barros, F. de V., Bittencourt, P. R. L., Brum, M., Restrepo-Coupe, N., Pereira, L., Teodoro, G. S., Saleska, S. R., Borma, L. S., Christoffersen, B. O., Penha, D., Alves, L. F., Lima, A. J. N., Carneiro, V. M. C., Gentine, P., Lee, J.-E., Aragão, L. E. O. C., Ivanov, V., Leal, L. S. M., Araujo, A. C., and Oliveira, R. S.: Hydraulic traits explain differential responses of Amazonian forests to the 2015 El Niño-induced drought, New Phytologist, 223, 1253–1266, https://doi.org/10.1111/nph.15909, 2019.

Bauman, D., Fortunel, C., Delhaye, G., Malhi, Y., Cernusak, L. A., Bentley, L. P., Rifai, S. W., Aguirre-Gutiérrez, J., Menor, I. O., Phillips, O. L., McNellis, B. E., Bradford, M., Laurance, S. G. W., Hutchinson, M. F., Dempsey, R., Santos-Andrade, P. E., Ninantay-Rivera, H. R., Chambi Paucar, J. R., and McMahon, S. M.: Tropical tree mortality has increased with rising atmospheric water stress, Nature, 1–6, https://doi.org/10.1038/s41586-022-04737-7, 2022.

de Boer-Euser, T., McMillan, H. K., Hrachowitz, M., Winsemius, H. C., and Savenije, H. H. G.: Influence of soil and climate on root zone storage capacity, Water Resources Research, 52, 2009–2024, https://doi.org/10.1002/2015WR018115, 2016.

Bouaziz, L. J. E., Steele-Dunne, S. C., Schellekens, J., Weerts, A. H., Stam, J., Sprokkereef, E., Winsemius, H. H. C., Savenije, H. H. G., and Hrachowitz, M.: Improved Understanding of the Link Between Catchment-Scale Vegetation Accessible Storage and Satellite-Derived Soil Water Index, Water Resources Research, 56, e2019WR026365, https://doi.org/10.1029/2019WR026365, 2020.

Boulton, C. A., Good, P., and Lenton, T. M.: Early warning signals of simulated Amazon rainforest dieback, Theor Ecol, 6, 373–384, https://doi.org/10.1007/s12080-013-0191-7, 2013.

Boulton, C. A., Booth, B. B. B., and Good, P.: Exploring uncertainty of Amazon dieback in a perturbed parameter Earth system ensemble, Global Change Biology, 23, 5032–5044, https://doi.org/10.1111/gcb.13733, 2017.

Boulton, C. A., Lenton, T. M., and Boers, N.: Pronounced loss of Amazon rainforest resilience since the early 2000s, Nat. Clim. Chang., 12, 271–278, https://doi.org/10.1038/s41558-022-01287-8, 2022.

Bovolo, C. I., Wagner, T., Parkin, G., Hein-Griggs, D., Pereira, R., and Jones, R.: The Guiana Shield rainforests— overlooked guardians of South American climate, Environ. Res. Lett., 13, 074029, https://doi.org/10.1088/1748-9326/aacf60, 2018.

Brienen, R. J. W., Phillips, O. L., Feldpausch, T. R., Gloor, E., Baker, T. R., Lloyd, J., Lopez-Gonzalez, G., Monteagudo-Mendoza, A., Malhi, Y., Lewis, S. L., Vásquez Martinez, R., Alexiades, M., Álvarez Dávila, E., Alvarez-Loayza, P., Andrade, A., Aragão, L. E. O. C., Araujo-Murakami, A., Arets, E. J. M. M., Arroyo, L., Aymard C., G. A., Bánki, O. S., Baraloto, C., Barroso, J., Bonal, D., Boot, R. G. A., Camargo, J. L. C., Castilho, C. V., Chama, V., Chao, K. J., Chave, J., Comiskey, J. A., Cornejo Valverde, F., da Costa, L., de Oliveira, E. A., Di Fiore, A., Erwin, T. L., Fauset, S., Forsthofer, M., Galbraith, D. R., Grahame, E. S., Groot, N., Hérault, B., Higuchi, N., Honorio Coronado, E. N., Keeling, H., Killeen, T. J., Laurance, W. F., Laurance, S., Licona, J., Magnussen, W. E., Marimon, B. S., Marimon-Junior, B. H., Mendoza, C., Neill, D. A., Nogueira, E. M., Núñez, P., Pallqui Camacho, N. C., Parada, A., Pardo-Molina, G., Peacock, J., Peña-Claros, M., Pickavance, G. C., Pitman, N. C. A., Poorter, L., Prieto, A., Quesada, C. A., Ramírez, F., Ramírez-Angulo, H., Restrepo, Z., Roopsind, A., Rudas, A., Salomão, R. P., Schwarz, M., Silva, N., Silva-Espejo, J. E., Silveira, M., Stropp, J., Talbot, J., ter Steege, H., Teran-Aguilar, J., Terborgh, J., Thomas-Caesar, R., Toledo, M., Torello-Raventos, M., Umetsu, R. K., van der Heijden, G. M. F., van der Hout, P., Guimarães Vieira, I. C., Vieira, S. A., Vilanova, E., Vos, V. A., and Zagt, R. J.: Long-term decline of the Amazon carbon sink, Nature, 519, 344–348, https://doi.org/10.1038/nature14283, 2015.

Bronick, C. J. and Lal, R.: Soil structure and management: a review, Geoderma, 124, 3–22, https://doi.org/10.1016/j.geoderma.2004.03.005, 2005.

Brooks, P. D., Chorover, J., Fan, Y., Godsey, S. E., Maxwell, R. M., McNamara, J. P., and Tague, C.: Hydrological partitioning in the critical zone: Recent advances and opportunities for developing transferable understanding of water cycle dynamics, Water Resources Research, 51, 6973–6987, https://doi.org/10.1002/2015WR017039, 2015.

Brum, M., Vadeboncoeur, M. A., Ivanov, V., Asbjornsen, H., Saleska, S., Alves, L. F., Penha, D., Dias, J. D., Aragão, L. E. O. C., Barros, F., Bittencourt, P., Pereira, L., and Oliveira, R. S.: Hydrological niche segregation defines forest structure and drought tolerance strategies in a seasonal Amazon forest, Journal of Ecology, 107, 318–333, https://doi.org/10.1111/1365-2745.13022, 2019.

Brunner, I., Herzog, C., Dawes, M. A., Arend, M., and Sperisen, C.: How tree roots respond to drought, Frontiers in Plant Science, 6, 2015.

Bruno, R. D., Rocha, H. R. da, Freitas, H. C. de, Goulden, M. L., and Miller, S. D.: Soil moisture dynamics in an eastern Amazonian tropical forest, Hydrological Processes, 20, 2477–2489, https://doi.org/10.1002/hyp.6211, 2006.

Canadell, J., Jackson, R. B., Ehleringer, J. B., Mooney, H. A., Sala, O. E., and Schulze, E.-D.: Maximum rooting depth of vegetation types at the global scale, Oecologia, 108, 583–595, https://doi.org/10.1007/BF00329030, 1996.

Canadell, J. G., Monteiro, P. M. S., Costa, M. H., Cunha, L. C. D., Cox, P. M., Eliseev, A. V., Henson, S., Ishii, M., Jaccard, S., Koven, C., Lohila, A., Patra, P. K., Piao, S., Syampungani, S., Zaehle, S., Zickfeld, K., Alexandrov, G. A., Bala, G., Bopp, L., Boysen, L., Cao, L., Chandra, N., Ciais, P., Denisov, S. N., Dentener, F. J., Douville, H., Fay,

799   A., Forster, P., Fox-Kemper, B., Friedlingstein, P., Fu, W., Fuss, S., Garçon, V., Gier, B., Gillett, N. P., Gregor, L.,
800   Haustein, K., Haverd, V., He, J., Hewitt, H. T., Hoffman, F. M., Ilyina, T., Jackson, R., Jones, C., Keller, D. P.,
801   Kwiatkowski, L., Lamboll, R. D., Lan, X., Laufkötter, C., Quéré, C. L., Lenton, A., Lewis, J., Liddicoat, S.,
802   Lorenzoni, L., Lovenduski, N., Macdougall, A. H., Mathesius, S., Matthews, D. H., Meinshausen, M., Mokhov, I.
803   I., Naik, V., Nicholls, Z. R. J., Nurhati, I. S., O'sullivan, M., Peters, G., Pongratz, J., Poulter, B., Sallée, J.-B.,
804   Saunois, M., Schuur, E. A. G., I.Seneviratne, S., Stavert, A., Suntharalingam, P., Tachiiri, K., Terhaar, J.,
805   Thompson, R., Tian, H., Turnbull, J., Vicente-Serrano, S. M., Wang, X., Wanninkhof, R. H., Williamson, P.,
806   Brovkin, V., Feely, R. A., and Lebehot, A. D.: Global Carbon and other Biogeochemical Cycles and Feedbacks,
807   in: IPCC AR6 WGI, Final Government Distribution, chapter 5, 2021.

808   Chai, Y., Martins, G., Nobre, C., von Randow, C., Chen, T., and Dolman, H.: Constraining Amazonian land
809   surface temperature sensitivity to precipitation and the probability of forest dieback, npj Clim Atmos Sci, 4, 1–
810   7, https://doi.org/10.1038/s41612-021-00162-1, 2021.

811   Cheng, S., Huang, J., Ji, F., and Lin, L.: Uncertainties of soil moisture in historical simulations and future
812   projections, Journal of Geophysical Research: Atmospheres, 122, 2239–2253,
813   https://doi.org/10.1002/2016JD025871, 2017.

814   Cole, L. E. S., Bhagwat, S. A., and Willis, K. J.: Recovery and resilience of tropical forests after disturbance,
815   Nature Communications, 5, 3906, https://doi.org/10.1038/ncomms4906, 2014.

816   Condit, R., Engelbrecht, B. M. J., Pino, D., Pérez, R., and Turner, B. L.: Species distributions in response to
817   individual soil nutrients and seasonal drought across a community of tropical trees, PNAS, 110, 5064–5068,
818   https://doi.org/10.1073/pnas.1218042110, 2013.

819   Cook, K. H. and Vizy, E. K.: Impact of climate change on mid-twenty-first century growing seasons in Africa,
820   Clim Dyn, 39, 2937–2955, https://doi.org/10.1007/s00382-012-1324-1, 2012.

821   Cooper, G. S., Willcock, S., and Dearing, J. A.: Regime shifts occur disproportionately faster in larger
822   ecosystems, Nature Communications, 11, 1175, https://doi.org/10.1038/s41467-020-15029-x, 2020.

823   skextremes Documentation: https://github.com/kikocorreoso/scikit-extremes.

824   Cox, P. M., Betts, R. A., Collins, M., Harris, P. P., Huntingford, C., and Jones, C. D.: Amazonian forest dieback
825   under climate-carbon cycle projections for the 21st century, Theor Appl Climatol, 78, 137–156,
826   https://doi.org/10.1007/s00704-004-0049-4, 2004.

827   Dai, A.: Drought under global warming: a review, WIREs Climate Change, 2, 45–65,
828   https://doi.org/10.1002/wcc.81, 2011.

829   Davidson, E. A., de Araújo, A. C., Artaxo, P., Balch, J. K., Brown, I. F., C. Bustamante, M. M., Coe, M. T., DeFries,
830   R. S., Keller, M., Longo, M., Munger, J. W., Schroeder, W., Soares-Filho, B. S., Souza, C. M., and Wofsy, S. C.:
831   The Amazon basin in transition, Nature, 481, 321–328, https://doi.org/10.1038/nature10717, 2012.

832   Dexter, A. R.: Soil physical quality: Part II. Friability, tillage, tilth and hard-setting, Geoderma, 120, 215–225,
833   https://doi.org/10.1016/j.geoderma.2003.09.005, 2004.

834   Dittert, K., Wätzel, J., and Sattelmacher, B.: Responses of Alnus glutinosa to Anaerobic Conditions -
835   Mechanisms and Rate of Oxygen Flux into the Roots, Plant Biology, 8, 212–223, https://doi.org/10.1055/s-
836   2005-873041, 2006.

837   Doughty, C. E., Keany, J. M., Wiebe, B. C., Rey-Sanchez, C., Carter, K. R., Middleby, K. B., Cheesman, A. W.,
838   Goulden, M. L., da Rocha, H. R., Miller, S. D., Malhi, Y., Fauset, S., Gloor, E., Slot, M., Oliveras Menor, I., Crous,

839   K. Y., Goldsmith, G. R., and Fisher, J. B.: Tropical forests are approaching critical temperature thresholds,
840   Nature, 621, 105–111, https://doi.org/10.1038/s41586-023-06391-z, 2023.

841   Drijfhout, S., Bathiany, S., Beaulieu, C., Brovkin, V., Claussen, M., Huntingford, C., Scheffer, M., Sgubin, G., and
842   Swingedouw, D.: Catalogue of abrupt shifts in Intergovernmental Panel on Climate Change climate models,
843   Proceedings of the National Academy of Sciences, 112, E5777–E5786,
844   https://doi.org/10.1073/pnas.1511451112, 2015.

845   Dunning, C. M., Black, E., and Allan, R. P.: Later Wet Seasons with More Intense Rainfall over Africa under
846   Future Climate Change, Journal of Climate, 31, 9719–9738, 2018.

847   van der Ent, R. J., Savenije, H. H. G., Schaefli, B., and Steele-Dunne, S. C.: Origin and fate of atmospheric
848   moisture over continents, Water Resources Research, 46, https://doi.org/10.1029/2010WR009127, 2010.

849   GlobCover land-use map: http://due.esrin.esa.int/page_globcover.php, last access: 27 February 2022.

850   Esquivel-Muelbert, A., Baker, T. R., Dexter, K. G., Lewis, S. L., Brienen, R. J. W., Feldpausch, T. R., Lloyd, J.,
851   Monteagudo-Mendoza, A., Arroyo, L., Álvarez-Dávila, E., Higuchi, N., Marimon, B. S., Marimon-Junior, B. H.,
852   Silveira, M., Vilanova, E., Gloor, E., Malhi, Y., Chave, J., Barlow, J., Bonal, D., Cardozo, N. D., Erwin, T., Fauset,
853   S., Hérault, B., Laurance, S., Poorter, L., Qie, L., Stahl, C., Sullivan, M. J. P., Steege, H. ter, Vos, V. A., Zuidema,
854   P. A., Almeida, E., Oliveira, E. A. de, Andrade, A., Vieira, S. A., Aragão, L., Araujo-Murakami, A., Arets, E., C, G.
855   A. A., Baraloto, C., Camargo, P. B., Barroso, J. G., Bongers, F., Boot, R., Camargo, J. L., Castro, W., Moscoso, V.
856   C., Comiskey, J., Valverde, F. C., Costa, A. C. L. da, Pasquel, J. del A., Fiore, A. D., Duque, L. F., Elias, F., Engel, J.,
857   Llampazo, G. F., Galbraith, D., Fernández, R. H., Coronado, E. H., Hubau, W., Jimenez-Rojas, E., Lima, A. J. N.,
858   Umetsu, R. K., Laurance, W., Lopez-Gonzalez, G., Lovejoy, T., Cruz, O. A. M., Morandi, P. S., Neill, D., Vargas, P.
859   N., Camacho, N. C. P., Gutierrez, A. P., Pardo, G., Peacock, J., Peña-Claros, M., Peñuela-Mora, M. C., Petronelli,
860   P., Pickavance, G. C., Pitman, N., Prieto, A., Quesada, C., Ramírez-Angulo, H., Réjou-Méchain, M., Correa, Z. R.,
861   Roopsind, A., Rudas, A., Salomão, R., Silva, N., Espejo, J. S., Singh, J., Stropp, J., Terborgh, J., Thomas, R.,
862   Toledo, M., Torres-Lezama, A., Gamarra, L. V., Meer, P. J. van de, Heijden, G. van der, et al.: Compositional
863   response of Amazon forests to climate change, Global Change Biology, 25, 39–56,
864   https://doi.org/10.1111/gcb.14413, 2019.

865   Fan, Y., Miguez-Macho, G., Jobbágy, E. G., Jackson, R. B., and Otero-Casal, C.: Hydrologic regulation of plant
866   rooting depth, Proceedings of the National Academy of Sciences, 114, 10572–10577,
867   https://doi.org/10.1073/pnas.1712381114, 2017.

868   Fayos, C. B.: The roles of texture and structure in the water retention capacity of burnt Mediterranean soils
869   with varying rainfall, CATENA, 31, 219–236, https://doi.org/10.1016/S0341-8162(97)00041-6, 1997.

870   Ferreira, D., Marshall, J., and Rose, B.: Climate Determinism Revisited: Multiple Equilibria in a Complex
871   Climate Model, Journal of Climate, 24, 992–1012, https://doi.org/10.1175/2010JCLI3580.1, 2011.

872   Fleischer, K., Rammig, A., De Kauwe, M. G., Walker, A. P., Domingues, T. F., Fuchslueger, L., Garcia, S., Goll, D.
873   S., Grandis, A., Jiang, M., Haverd, V., Hofhansl, F., Holm, J. A., Kruijt, B., Leung, F., Medlyn, B. E., Mercado, L.
874   M., Norby, R. J., Pak, B., von Randow, C., Quesada, C. A., Schaap, K. J., Valverde-Barrantes, O. J., Wang, Y.-P.,
875   Yang, X., Zaehle, S., Zhu, Q., and Lapola, D. M.: Amazon forest response to CO2 fertilization dependent on
876   plant phosphorus acquisition, Nat. Geosci., 12, 736–741, https://doi.org/10.1038/s41561-019-0404-9, 2019.

877   Flores, B. M., Montoya, E., Sakschewski, B., Nascimento, N., Staal, A., Betts, R. A., Levis, C., Lapola, D. M.,
878   Esquível-Muelbert, A., Jakovac, C., Nobre, C. A., Oliveira, R. S., Borma, L. S., Nian, D., Boers, N., Hecht, S. B., ter
879   Steege, H., Arieira, J., Lucas, I. L., Berenguer, E., Marengo, J. A., Gatti, L. V., Mattos, C. R. C., and Hirota, M.:
880   Critical transitions in the Amazon forest system, Nature, 626, 555–564, https://doi.org/10.1038/s41586-023-
881   06970-0, 2024.

Funk, C., Peterson, P., Landsfeld, M., Pedreros, D., Verdin, J., Shukla, S., Husak, G., Rowland, J., Harrison, L., Hoell, A., and Michaelsen, J.: The climate hazards infrared precipitation with stations—a new environmental record for monitoring extremes, Scientific Data, 2, 150066, https://doi.org/10.1038/sdata.2015.66, 2015.

Gao, H., Hrachowitz, M., Schymanski, S. J., Fenicia, F., Sriwongsitanon, N., and Savenije, H. H. G.: Climate controls how ecosystems size the root zone storage capacity at catchment scale: Root zone storage capacity in catchments, Geophysical Research Letters, 41, 7916–7923, https://doi.org/10.1002/2014GL061668, 2014.

Grimm, N. B., Chapin III, F. S., Bierwagen, B., Gonzalez, P., Groffman, P. M., Luo, Y., Melton, F., Nadelhoffer, K., Pairis, A., Raymond, P. A., Schimel, J., and Williamson, C. E.: The impacts of climate change on ecosystem structure and function, Frontiers in Ecology and the Environment, 11, 474–482, https://doi.org/10.1890/120282, 2013.

Gumbel, E. J.: Statistics of extremes., Columbia University Press, New York, 1958.

Guswa, A. J.: The influence of climate on root depth: A carbon cost-benefit analysis, Water Resources Research, 44, W02427, https://doi.org/10.1029/2007WR006384, 2008.

Hahm, W. J., Rempe, D. M., Dralle, D. N., Dawson, T. E., Lovill, S. M., Bryk, A. B., Bish, D. L., Schieber, J., and Dietrich, W. E.: Lithologically Controlled Subsurface Critical Zone Thickness and Water Storage Capacity Determine Regional Plant Community Composition, Water Resources Research, 55, 3028–3055, https://doi.org/10.1029/2018WR023760, 2019.

Hall, A., Cox, P., Huntingford, C., and Klein, S.: Progressing emergent constraints on future climate change, Nat. Clim. Chang., 9, 269–278, https://doi.org/10.1038/s41558-019-0436-6, 2019.

Hersbach, H., Bell, B., Berrisford, P., Hirahara, S., Horányi, A., Muñoz-Sabater, J., Nicolas, J., Peubey, C., Radu, R., Schepers, D., Simmons, A., Soci, C., Abdalla, S., Abellan, X., Balsamo, G., Bechtold, P., Biavati, G., Bidlot, J., Bonavita, M., Chiara, G. D., Dahlgren, P., Dee, D., Diamantakis, M., Dragani, R., Flemming, J., Forbes, R., Fuentes, M., Geer, A., Haimberger, L., Healy, S., Hogan, R. J., Hólm, E., Janisková, M., Keeley, S., Laloyaux, P., Lopez, P., Lupu, C., Radnoti, G., Rosnay, P. de, Rozum, I., Vamborg, F., Villaume, S., and Thépaut, J.-N.: The ERA5 Global Reanalysis, Quarterly Journal of the Royal Meteorological Society, 245, 111840, https://doi.org/10.1002/qj.3803, 2020.

Higgins, S. I. and Scheiter, S.: Atmospheric CO2 forces abrupt vegetation shifts locally, but not globally, Nature, 488, 209–212, https://doi.org/10.1038/nature11238, 2012.

Hildebrandt, A., Kleidon, A., and Bechmann, M.: A thermodynamic formulation of root water uptake, Hydrology and Earth System Sciences, 20, 3441–3454, https://doi.org/10.5194/hess-20-3441-2016, 2016.

Hirota, M., Holmgren, M., Van Nes, E. H., and Scheffer, M.: Global Resilience of Tropical Forest and Savanna to Critical Transitions, Science, 334, 232–235, https://doi.org/10.1126/science.1210657, 2011.

Hirota, M., Flores, B. M., Betts, R., Borma, L. S., Esquivel-Muelbert, A., Jakovac, C., Lapola, D. M., Montoya, E., Oliveira, R. S., and Sakschewski, B.: Chapter 24: Resilience of the Amazon forest to global changes: Assessing the risk of tipping points, in: Amazon Assessment Report 2021, edited by: Nobre, C., Encalada, A., Anderson, E., Roca Alcazar, F. H., Bustamante, M., Mena, C., Peña-Claros, M., Poveda, G., Rodriguez, J. P., Saleska, S., Trumbore, S. E., Val, A., Villa Nova, L., Abramovay, R., Alencar, A., Rodriguez Alzza, A. C., Armenteras, D., Artaxo, P., Athayde, S., Barretto Filho, H. T., Barlow, J., Berenguer, E., Bortolotto, F., Costa, F. de A., Costa, M. H., Cuvi, N., Fearnside, P., Ferreira, J., Flores, B. M., Frieri, S., Gatti, L. V., Guayasamin, J. M., Hecht, S., Hirota, M., Hoorn, C., Josse, C., Lapola, D. M., Larrea, C., Larrea-Alcazar, D. M., Lehm Ardaya, Z., Malhi, Y., Marengo, J. A., Melack, J., Moraes R., M., Moutinho, P., Murmis, M. R., Neves, E. G., Paez, B., Painter, L., Ramos, A.,

Rosero-Peña, M. C., Schmink, M., Sist, P., ter Steege, H., Val, P., van der Voort, H., Varese, M., and Zapata-Ríos, G., UN Sustainable Development Solutions Network (SDSN), https://doi.org/10.55161/QPYS9758, 2021.

Hofhansl, F., Andersen, K. M., Fleischer, K., Fuchslueger, L., Rammig, A., Schaap, K. J., Valverde-Barrantes, O. J., and Lapola, D. M.: Amazon Forest Ecosystem Responses to Elevated Atmospheric CO_2 and Alterations in Nutrient Availability: Filling the Gaps with Model-Experiment Integration, Frontiers in Earth Science, 4, 2016.

Hubau, W., Lewis, S. L., Phillips, O. L., Affum-Baffoe, K., Beeckman, H., Cuní-Sanchez, A., Daniels, A. K., Ewango, C. E. N., Fauset, S., Mukinzi, J. M., Sheil, D., Sonké, B., Sullivan, M. J. P., Sunderland, T. C. H., Taedoumg, H., Thomas, S. C., White, L. J. T., Abernethy, K. A., Adu-Bredu, S., Amani, C. A., Baker, T. R., Banin, L. F., Baya, F., Begne, S. K., Bennett, A. C., Benedet, F., Bitariho, R., Bocko, Y. E., Boeckx, P., Boundja, P., Brienen, R. J. W., Brncic, T., Chezeaux, E., Chuyong, G. B., Clark, C. J., Collins, M., Comiskey, J. A., Coomes, D. A., Dargie, G. C., de Haulleville, T., Kamdem, M. N. D., Doucet, J.-L., Esquivel-Muelbert, A., Feldpausch, T. R., Fofanah, A., Foli, E. G., Gilpin, M., Gloor, E., Gonmadje, C., Gourlet-Fleury, S., Hall, J. S., Hamilton, A. C., Harris, D. J., Hart, T. B., Hockemba, M. B. N., Hladik, A., Ifo, S. A., Jeffery, K. J., Jucker, T., Yakusu, E. K., Kearsley, E., Kenfack, D., Koch, A., Leal, M. E., Levesley, A., Lindsell, J. A., Lisingo, J., Lopez-Gonzalez, G., Lovett, J. C., Makana, J.-R., Malhi, Y., Marshall, A. R., Martin, J., Martin, E. H., Mbayu, F. M., Medjibe, V. P., Mihindou, V., Mitchard, E. T. A., Moore, S., Munishi, P. K. T., Bengone, N. N., Ojo, L., Ondo, F. E., Peh, K. S.-H., Pickavance, G. C., Poulsen, A. D., Poulsen, J. R., Qie, L., Reitsma, J., Rovero, F., Swaine, M. D., Talbot, J., Taplin, J., Taylor, D. M., Thomas, D. W., Toirambe, B., Mukendi, J. T., Tuagben, D., Umunay, P. M., et al.: Asynchronous carbon sink saturation in African and Amazonian tropical forests, Nature, 579, 80–87, https://doi.org/10.1038/s41586-020-2035-0, 2020.

Huntingford, C., Zelazowski, P., Galbraith, D., Mercado, L. M., Sitch, S., Fisher, R., Lomas, M., Walker, A. P., Jones, C. D., Booth, B. B. B., Malhi, Y., Hemming, D., Kay, G., Good, P., Lewis, S. L., Phillips, O. L., Atkin, O. K., Lloyd, J., Gloor, E., Zaragoza-Castells, J., Meir, P., Betts, R., Harris, P. P., Nobre, C., Marengo, J., and Cox, P. M.: Simulated resilience of tropical rainforests to CO_2-induced climate change, Nature Geosci, 6, 268–273, https://doi.org/10.1038/ngeo1741, 2013.

Hurtt, G. C., Chini, L., Sahajpal, R., Frolking, S., Bodirsky, B. L., Calvin, K., Doelman, J. C., Fisk, J., Fujimori, S., Klein Goldewijk, K., Hasegawa, T., Havlik, P., Heinimann, A., Humpenöder, F., Jungclaus, J., Kaplan, J. O., Kennedy, J., Krisztin, T., Lawrence, D., Lawrence, P., Ma, L., Mertz, O., Pongratz, J., Popp, A., Poulter, B., Riahi, K., Shevliakova, E., Stehfest, E., Thornton, P., Tubiello, F. N., van Vuuren, D. P., and Zhang, X.: Harmonization of global land use change and management for the period 850–2100 (LUH2) for CMIP6, Geoscientific Model Development, 13, 5425–5464, https://doi.org/10.5194/gmd-13-5425-2020, 2020.

Indoria, A. K., Sharma, K. L., and Reddy, K. S.: Chapter 18 - Hydraulic properties of soil under warming climate, in: Climate Change and Soil Interactions, edited by: Prasad, M. N. V. and Pietrzykowski, M., Elsevier, 473–508, https://doi.org/10.1016/B978-0-12-818032-7.00018-7, 2020.

Jach, L., Warrach-Sagi, K., Ingwersen, J., Kaas, E., and Wulfmeyer, V.: Land Cover Impacts on Land-Atmosphere Coupling Strength in Climate Simulations With WRF Over Europe, Journal of Geophysical Research: Atmospheres, 125, e2019JD031989, https://doi.org/10.1029/2019JD031989, 2020.

Jackson, R. B., Canadell, J., Ehleringer, J. R., Mooney, H. A., Sala, O. E., and Schulze, E. D.: A global analysis of root distributions for terrestrial biomes, Oecologia, 108, 389–411, https://doi.org/10.1007/BF00333714, 1996.

Jehn, F. U., Kemp, L., Ilin, E., Funk, C., Wang, J. R., and Breuer, L.: Focus of the IPCC Assessment Reports Has Shifted to Lower Temperatures, Earth's Future, 10, e2022EF002876, https://doi.org/10.1029/2022EF002876, 2022.

Jiang, C. and Ryu, Y.: Multi-scale evaluation of global gross primary productivity and evapotranspiration products derived from Breathing Earth System Simulator (BESS), Remote Sensing of Environment, 186, 528–547, https://doi.org/10.1016/j.rse.2016.08.030, 2016.

Jones, C., Lowe, J., Liddicoat, S., and Betts, R.: Committed terrestrial ecosystem changes due to climate change, Nature Geosci, 2, 484–487, https://doi.org/10.1038/ngeo555, 2009.

Jung, M., Koirala, S., Weber, U., Ichii, K., Gans, F., Camps-Valls, G., Papale, D., Schwalm, C., Tramontana, G., and Reichstein, M.: The FLUXCOM ensemble of global land-atmosphere energy fluxes, Sci Data, 6, 74, https://doi.org/10.1038/s41597-019-0076-8, 2019.

Koch, A., Hubau, W., and Lewis, S. L.: Earth System Models Are Not Capturing Present-Day Tropical Forest Carbon Dynamics, Earth's Future, 9, e2020EF001874, https://doi.org/10.1029/2020EF001874, 2021.

Kooperman, G. J., Chen, Y., Hoffman, F. M., Koven, C. D., Lindsay, K., Pritchard, M. S., Swann, A. L. S., and Randerson, J. T.: Forest response to rising CO_2 drives zonally asymmetric rainfall change over tropical land, Nature Clim Change, 8, 434–440, https://doi.org/10.1038/s41558-018-0144-7, 2018.

Körner, C.: A matter of tree longevity, Science, 355, 130–131, https://doi.org/10.1126/science.aal2449, 2017.

Küçük, Ç., Koirala, S., Carvalhais, N., Miralles, D. G., Reichstein, M., and Jung, M.: Characterizing the Response of Vegetation Cover to Water Limitation in Africa Using Geostationary Satellites, Journal of Advances in Modeling Earth Systems, 14, e2021MS002730, https://doi.org/10.1029/2021MS002730, 2022.

Kukal, M. S. and Irmak, S.: Can limits of plant available water be inferred from soil moisture distributions?, Agricultural & Environmental Letters, 8, e20113, https://doi.org/10.1002/ael2.20113, 2023.

Lammertsma, E. I., Boer, H. J. de, Dekker, S. C., Dilcher, D. L., Lotter, A. F., and Wagner-Cremer, F.: Global CO_2 rise leads to reduced maximum stomatal conductance in Florida vegetation, PNAS, 108, 4035–4040, https://doi.org/10.1073/pnas.1100371108, 2011.

Lawrence, D., Coe, M., Walker, W., Verchot, L., and Vandecar, K.: The Unseen Effects of Deforestation: Biophysical Effects on Climate, Frontiers in Forests and Global Change, 5, 2022.

Leite-Filho, A. T., Soares-Filho, B. S., Davis, J. L., Abrahão, G. M., and Börner, J.: Deforestation reduces rainfall and agricultural revenues in the Brazilian Amazon, Nat Commun, 12, 2591, https://doi.org/10.1038/s41467-021-22840-7, 2021.

Lenton, T. M.: Early warning of climate tipping points, Nature Clim Change, 1, 201–209, https://doi.org/10.1038/nclimate1143, 2011.

Lenton, T. M., Rockström, J., Gaffney, O., Rahmstorf, S., Richardson, K., Steffen, W., and Schellnhuber, H. J.: Climate tipping points — too risky to bet against, Nature, 575, 592–595, https://doi.org/10.1038/d41586-019-03595-0, 2019.

Lewis, S. L., Edwards, D. P., and Galbraith, D.: Increasing human dominance of tropical forests, Science, 349, 827–832, https://doi.org/10.1126/science.aaa9932, 2015.

Li, Y., Brando, P. M., Morton, D. C., Lawrence, D. M., Yang, H., and Randerson, J. T.: Deforestation-induced climate change reduces carbon storage in remaining tropical forests, Nat Commun, 13, 1964, https://doi.org/10.1038/s41467-022-29601-0, 2022.

Liu, W., Sun, F., Lim, W. H., Zhang, J., Wang, H., Shiogama, H., and Zhang, Y.: Global drought and severe drought-affected populations in 1.5 and 2 °C warmer worlds, Earth System Dynamics, 9, 267–283, https://doi.org/10.5194/esd-9-267-2018, 2018.

Liu, Y., Kumar, M., Katul, G. G., Feng, X., and Konings, A. G.: Plant hydraulics accentuates the effect of atmospheric moisture stress on transpiration, Nat. Clim. Chang., 10, 691–695, https://doi.org/10.1038/s41558-020-0781-5, 2020.

Ma, L., Hurtt, G. C., Chini, L. P., Sahajpal, R., Pongratz, J., Frolking, S., Stehfest, E., Klein Goldewijk, K., O'Leary, D., and Doelman, J. C.: Global rules for translating land-use change (LUH2) to land-cover change for CMIP6 using GLM2, Geoscientific Model Development, 13, 3203–3220, https://doi.org/10.5194/gmd-13-3203-2020, 2020.

Malhi, Y., Roberts, J. T., Betts, R. A., Killeen, T. J., Li, W., and Nobre, C. A.: Climate Change, Deforestation, and the Fate of the Amazon, Science, 319, 169–172, https://doi.org/10.1126/science.1146961, 2008.

Malhi, Y., Gardner, T. A., Goldsmith, G. R., Silman, M. R., and Zelazowski, P.: Tropical Forests in the Anthropocene, Annu. Rev. Environ. Resour., 39, 125–159, https://doi.org/10.1146/annurev-environ-030713-155141, 2014.

Mamalakis, A., Randerson, J. T., Yu, J.-Y., Pritchard, M. S., Magnusdottir, G., Smyth, P., Levine, P. A., Yu, S., and Foufoula-Georgiou, E.: Zonally contrasting shifts of the tropical rain belt in response to climate change, Nature Climate Change, 11, 143–151, https://doi.org/10.1038/s41558-020-00963-x, 2021.

Maslin, M. and Austin, P.: Climate models at their limit?, Nature, 486, 183–184, https://doi.org/10.1038/486183a, 2012.

McCormick, E. L., Dralle, D. N., Hahm, W. J., Tune, A. K., Schmidt, L. M., Chadwick, K. D., and Rempe, D. M.: Widespread woody plant use of water stored in bedrock, Nature, 597, 225–229, https://doi.org/10.1038/s41586-021-03761-3, 2021.

McFarlane, N.: Parameterizations: representing key processes in climate models without resolving them, WIREs Climate Change, 2, 482–497, https://doi.org/10.1002/wcc.122, 2011.

Nepstad, D. C., Verssimo, A., Alencar, A., Nobre, C., Lima, E., Lefebvre, P., Schlesinger, P., Potter, C., Moutinho, P., Mendoza, E., Cochrane, M., and Brooks, V.: Large-scale impoverishment of Amazonian forests by logging and fire, Nature, 398, 505–508, https://doi.org/10.1038/19066, 1999.

van Nes, E. H., Arani, B. M. S., Staal, A., van der Bolt, B., Flores, B. M., Bathiany, S., and Scheffer, M.: What Do You Mean, 'Tipping Point'?, Trends in Ecology & Evolution, 31, 902–904, https://doi.org/10.1016/j.tree.2016.09.011, 2016.

Nijzink, R., Hutton, C., Pechlivanidis, I., Capell, R., Arheimer, B., Freer, J., Han, D., Wagener, T., McGuire, K., Savenije, H., and Hrachowitz, M.: The evolution of root-zone moisture capacities after deforestation: a step towards hydrological predictions under change?, Hydrology and Earth System Sciences, 20, 4775–4799, https://doi.org/10.5194/hess-20-4775-2016, 2016.

Nippert, J. B. and Holdo, R. M.: Challenging the maximum rooting depth paradigm in grasslands and savannas, Functional Ecology, 29, 739–745, https://doi.org/10.1111/1365-2435.12390, 2015.

Nof, D.: Simple Versus Complex Climate Modeling, Eos, Transactions American Geophysical Union, 89, 544–545, https://doi.org/10.1029/2008EO520006, 2008.

Oliveira, R. S., Dawson, T. E., Burgess, S. S. O., and Nepstad, D. C.: Hydraulic redistribution in three Amazonian trees, Oecologia, 145, 354–363, https://doi.org/10.1007/s00442-005-0108-2, 2005.

Parry, I. M., Ritchie, P. D. L., and Cox, P. M.: Evidence of localised Amazon rainforest dieback in CMIP6 models, Earth System Dynamics, 13, 1667–1675, https://doi.org/10.5194/esd-13-1667-2022, 2022.

Pascale, S., Carvalho, L. M. V., Adams, D. K., Castro, C. L., and Cavalcanti, I. F. A.: Current and Future Variations of the Monsoons of the Americas in a Warming Climate, Curr Clim Change Rep, 5, 125–144, https://doi.org/10.1007/s40641-019-00135-w, 2019.

Piani, C., Weedon, G. P., Best, M., Gomes, S. M., Viterbo, P., Hagemann, S., and Haerter, J. O.: Statistical bias correction of global simulated daily precipitation and temperature for the application of hydrological models, Journal of Hydrology, 395, 199–215, https://doi.org/10.1016/j.jhydrol.2010.10.024, 2010.

Poorter, L., Bongers, F., Aide, T. M., Almeyda Zambrano, A. M., Balvanera, P., Becknell, J. M., Boukili, V., Brancalion, P. H. S., Broadbent, E. N., Chazdon, R. L., Craven, D., de Almeida-Cortez, J. S., Cabral, G. A. L., de Jong, B. H. J., Denslow, J. S., Dent, D. H., DeWalt, S. J., Dupuy, J. M., Durán, S. M., Espírito-Santo, M. M., Fandino, M. C., César, R. G., Hall, J. S., Hernandez-Stefanoni, J. L., Jakovac, C. C., Junqueira, A. B., Kennard, D., Letcher, S. G., Licona, J.-C., Lohbeck, M., Marín-Spiotta, E., Martínez-Ramos, M., Massoca, P., Meave, J. A., Mesquita, R., Mora, F., Muñoz, R., Muscarella, R., Nunes, Y. R. F., Ochoa-Gaona, S., de Oliveira, A. A., Orihuela-Belmonte, E., Peña-Claros, M., Pérez-García, E. A., Piotto, D., Powers, J. S., Rodríguez-Velázquez, J., Romero-Pérez, I. E., Ruíz, J., Saldarriaga, J. G., Sanchez-Azofeifa, A., Schwartz, N. B., Steininger, M. K., Swenson, N. G., Toledo, M., Uriarte, M., van Breugel, M., van der Wal, H., Veloso, M. D. M., Vester, H. F. M., Vicentini, A., Vieira, I. C. G., Bentos, T. V., Williamson, G. B., and Rozendaal, D. M. A.: Biomass resilience of Neotropical secondary forests, Nature, 530, 211–214, https://doi.org/10.1038/nature16512, 2016.

Rammig, A.: Tropical carbon sinks are saturating at different times on different continents, Nature, 579, 38–39, https://doi.org/10.1038/d41586-020-00423-8, 2020.

Reyer, C. P. O., Brouwers, N., Rammig, A., Brook, B. W., Epila, J., Grant, R. F., Holmgren, M., Langerwisch, F., Leuzinger, S., Lucht, W., Medlyn, B., Pfeifer, M., Steinkamp, J., Vanderwel, M. C., Verbeeck, H., and Villela, D. M.: Forest resilience and tipping points at different spatio-temporal scales: approaches and challenges, Journal of Ecology, 103, 5–15, https://doi.org/10.1111/1365-2745.12337, 2015.

Rosas, T., Mencuccini, M., Barba, J., Cochard, H., Saura-Mas, S., and Martínez-Vilalta, J.: Adjustments and coordination of hydraulic, leaf and stem traits along a water availability gradient, New Phytologist, 223, 632–646, https://doi.org/10.1111/nph.15684, 2019.

Schenk, H. J.: Soil depth, plant rooting strategies and species' niches, New Phytologist, 178, 223–225, https://doi.org/10.1111/j.1469-8137.2008.02427.x, 2008.

Schenk, H. J. and Jackson, R. B.: The Global Biogeography of Roots, Ecological Monographs, 72, 311–328, https://doi.org/10.1890/0012-9615(2002)072[0311:TGBOR]2.0.CO;2, 2002.

Schumacher, D. L., Keune, J., Dirmeyer, P., and Miralles, D. G.: Drought self-propagation in drylands due to land–atmosphere feedbacks, Nat. Geosci., 15, 262–268, https://doi.org/10.1038/s41561-022-00912-7, 2022.

Singh, C.: Rooting for forest resilience : Implications of climate and land-use change on the tropical rainforests, 2023.

Singh, C., Wang-Erlandsson, L., Fetzer, I., Rockström, J., and van der Ent, R.: Rootzone storage capacity reveals drought coping strategies along rainforest-savanna transitions, Environ. Res. Lett., 15, 124021, https://doi.org/10.1088/1748-9326/abc377, 2020.

Singh, C., van der Ent, R., Wang-Erlandsson, L., and Fetzer, I.: Hydroclimatic adaptation critical to the resilience of tropical forests, Global Change Biology, 28, 2930–2939, https://doi.org/10.1111/gcb.16115, 2022.

Slik, J. W. F., Franklin, J., Arroyo-Rodríguez, V., Field, R., Aguilar, S., Aguirre, N., Ahumada, J., Aiba, S.-I., Alves, L. F., K, A., Avella, A., Mora, F., Aymard C., G. A., Báez, S., Balvanera, P., Bastian, M. L., Bastin, J.-F., Bellingham, P. J., van den Berg, E., da Conceição Bispo, P., Boeckx, P., Boehning-Gaese, K., Bongers, F., Boyle, B., Brambach, F., Brearley, F. Q., Brown, S., Chai, S.-L., Chazdon, R. L., Chen, S., Chhang, P., Chuyong, G., Ewango, C., Coronado, I. M., Cristóbal-Azkarate, J., Culmsee, H., Damas, K., Dattaraja, H. S., Davidar, P., DeWalt, S. J., Din, H., Drake, D. R., Duque, A., Durigan, G., Eichhorn, K., Eler, E. S., Enoki, T., Ensslin, A., Fandohan, A. B., Farwig, N., Feeley, K. J., Fischer, M., Forshed, O., Garcia, Q. S., Garkoti, S. C., Gillespie, T. W., Gillet, J.-F., Gonmadje, C., Granzow-de la Cerda, I., Griffith, D. M., Grogan, J., Hakeem, K. R., Harris, D. J., Harrison, R. D., Hector, A., Hemp, A., Homeier, J., Hussain, M. S., Ibarra-Manríquez, G., Hanum, I. F., Imai, N., Jansen, P. A., Joly, C. A., Joseph, S., Kartawinata, K., Kearsley, E., Kelly, D. L., Kessler, M., Killeen, T. J., Kooyman, R. M., Laumonier, Y., Laurance, S. G., Laurance, W. F., Lawes, M. J., Letcher, S. G., Lindsell, J., Lovett, J., Lozada, J., Lu, X., Lykke, A. M., Mahmud, K. B., Mahayani, N. P. D., Mansor, A., Marshall, A. R., Martin, E. H., Calderado Leal Matos, D., Meave, J. A., Melo, F. P. L., Mendoza, Z. H. A., et al.: Phylogenetic classification of the world's tropical forests, Proceedings of the National Academy of Sciences, 115, 1837–1842, https://doi.org/10.1073/pnas.1714977115, 2018.

Smith, C. W., Johnston, M. A., and Lorentz, S. A.: The effect of soil compaction on the water retention characteristics of soils in forest plantations, South African Journal of Plant and Soil, 18, 87–97, https://doi.org/10.1080/02571862.2001.10634410, 2001.

Staal, A., Tuinenburg, O. A., Bosmans, J. H. C., Holmgren, M., van Nes, E. H., Scheffer, M., Zemp, D. C., and Dekker, S. C.: Forest-rainfall cascades buffer against drought across the Amazon, Nature Climate Change, 8, 539–543, https://doi.org/10.1038/s41558-018-0177-y, 2018.

Staal, A., Fetzer, I., Wang-Erlandsson, L., Bosmans, J. H. C., Dekker, S. C., van Nes, E. H., Rockström, J., and Tuinenburg, O. A.: Hysteresis of tropical forests in the 21st century, Nat Commun, 11, 4978, https://doi.org/10.1038/s41467-020-18728-7, 2020.

Stevens, B. and Bony, S.: What Are Climate Models Missing?, Science, 340, 1053–1054, https://doi.org/10.1126/science.1237554, 2013.

Still, C. J., Berry, J. A., Collatz, G. J., and DeFries, R. S.: Global distribution of C3 and C4 vegetation: Carbon cycle implications, Global Biogeochemical Cycles, 17, 6-1-6–14, https://doi.org/10.1029/2001GB001807, 2003.

Stocker, B. D., Tumber-Dávila, S. J., Konings, A. G., Anderson, M. C., Hain, C., and Jackson, R. B.: Global patterns of water storage in the rooting zones of vegetation, Nat. Geosci., 1–7, https://doi.org/10.1038/s41561-023-01125-2, 2023.

Sveen, T. R., Hannula, S. E., and Bahram, M.: Microbial regulation of feedbacks to ecosystem change, Trends in Microbiology, 32, 68–78, https://doi.org/10.1016/j.tim.2023.06.006, 2024.

Trumbore, S., Brando, P., and Hartmann, H.: Forest health and global change, Science, 349, 814–818, https://doi.org/10.1126/science.aac6759, 2015.

Valdes, P.: Built for stability, Nature Geosci, 4, 414–416, https://doi.org/10.1038/ngeo1200, 2011.

Wang, E., Smith, C. J., Wang, E., and Smith, C. J.: Modelling the growth and water uptake function of plant root systems: a review, Aust. J. Agric. Res., 55, 501–523, https://doi.org/10.1071/AR03201, 2004.

Wang-Erlandsson, L., Bastiaanssen, W. G. M., Gao, H., Jägermeyr, J., Senay, G. B., van Dijk, A. I. J. M., Guerschman, J. P., Keys, P. W., Gordon, L. J., and Savenije, H. H. G.: Global root zone storage capacity from satellite-based evaporation, Hydrology and Earth System Sciences, 20, 1459–1481, https://doi.org/10.5194/hess-20-1459-2016, 2016.

Wang-Erlandsson, L., Tobian, A., van der Ent, R. J., Fetzer, I., te Wierik, S., Porkka, M., Staal, A., Jaramillo, F., Dahlmann, H., Singh, C., Greve, P., Gerten, D., Keys, P. W., Gleeson, T., Cornell, S. E., Steffen, W., Bai, X., and Rockström, J.: A planetary boundary for green water, Nat Rev Earth Environ, 3, 380–392, https://doi.org/10.1038/s43017-022-00287-8, 2022.

Wolfe, B. T., Sperry, J. S., and Kursar, T. A.: Does leaf shedding protect stems from cavitation during seasonal droughts? A test of the hydraulic fuse hypothesis, New Phytologist, 212, 1007–1018, https://doi.org/10.1111/nph.14087, 2016.

Wunderling, N., Staal, A., Sakschewski, B., Hirota, M., Tuinenburg, O. A., Donges, J. F., Barbosa, H. M. J., and Winkelmann, R.: Recurrent droughts increase risk of cascading tipping events by outpacing adaptive capacities in the Amazon rainforest, Proceedings of the National Academy of Sciences, 119, e2120777119, https://doi.org/10.1073/pnas.2120777119, 2022.

Xie, S.-P., Deser, C., Vecchi, G. A., Ma, J., Teng, H., and Wittenberg, A. T.: Global Warming Pattern Formation: Sea Surface Temperature and Rainfall, Journal of Climate, 23, 966–986, https://doi.org/10.1175/2009JCLI3329.1, 2010.

Xu, C., Hantson, S., Holmgren, M., van Nes, E. H., Staal, A., and Scheffer, M.: Remotely sensed canopy height reveals three pantropical ecosystem states, Ecology, 97, 2518–2521, https://doi.org/10.1002/ecy.1470, 2016.

Xue, B.-L., Guo, Q., Otto, A., Xiao, J., Tao, S., and Li, L.: Global patterns, trends, and drivers of water use efficiency from 2000 to 2013, Ecosphere, 6, art174, https://doi.org/10.1890/ES14-00416.1, 2015.

Yang, Y., Saatchi, S. S., Xu, L., Yu, Y., Choi, S., Phillips, N., Kennedy, R., Keller, M., Knyazikhin, Y., and Myneni, R. B.: Post-drought decline of the Amazon carbon sink, Nat Commun, 9, 3172, https://doi.org/10.1038/s41467-018-05668-6, 2018.

Yu, Z., Chen, X., Zhou, G., Agathokleous, E., Li, L., Liu, Z., Wu, J., Zhou, P., Xue, M., Chen, Y., Yan, W., Liu, L., Shi, T., and Zhao, X.: Natural forest growth and human induced ecosystem disturbance influence water yield in forests, Commun Earth Environ, 3, 148, https://doi.org/10.1038/s43247-022-00483-w, 2022.

Yuan, K., Zhu, Q., Riley, W. J., Li, F., and Wu, H.: Understanding and reducing the uncertainties of land surface energy flux partitioning within CMIP6 land models, Agricultural and Forest Meteorology, 319, 108920, https://doi.org/10.1016/j.agrformet.2022.108920, 2022.

Zemp, D. C., Schleussner, C.-F., Barbosa, H. M. J., van der Ent, R. J., Donges, J. F., Heinke, J., Sampaio, G., and Rammig, A.: On the importance of cascading moisture recycling in South America, Atmospheric Chemistry and Physics, 14, 13337–13359, https://doi.org/10.5194/acp-14-13337-2014, 2014.

Zemp, D. C., Schleussner, C.-F., Barbosa, H. M. J., Hirota, M., Montade, V., Sampaio, G., Staal, A., Wang-Erlandsson, L., and Rammig, A.: Self-amplified Amazon forest loss due to vegetation-atmosphere feedbacks, Nature Communications, 8, 14681, https://doi.org/10.1038/ncomms14681, 2017.

Zhang, Y., Peña-Arancibia, J. L., McVicar, T. R., Chiew, F. H. S., Vaze, J., Liu, C., Lu, X., Zheng, H., Wang, Y., Liu, Y. Y., Miralles, D. G., and Pan, M.: Multi-decadal trends in global terrestrial evapotranspiration and its components, Scientific Reports, 6, 19124, https://doi.org/10.1038/srep19124, 2016.

1164   Zilli, M. T., Carvalho, L. M. V., and Lintner, B. R.: The poleward shift of South Atlantic Convergence Zone in
1165   recent decades, Clim Dyn, 52, 2545–2563, https://doi.org/10.1007/s00382-018-4277-1, 2019.

1166